

Rothamsted Repository Download

A - Papers appearing in refereed journals

Garaycochea, S., Altier, N., Leoni, C., Neal, A. L. and Romero, H. 2022. Abundance and phylogenetic distribution of eight key enzymes of the phosphorus biogeochemical cycle in grassland soils. *Environmental Microbiology*. <https://doi.org/10.1111/1758-2229.13159> This is an open access article under the terms of the Creative Commons Attribution License, which permits use, distribution and reproduction in any medium, provided the original work is properly cited. ©2023 The Authors. Environmental Microbiology Reports published by Applied Microbiology International and John Wiley & Sons Ltd. Environmental Microbiology Reports. 2023; 1–18. wileyonlinelibrary.com/journal/emi41

The publisher's version can be accessed at:

- <https://doi.org/10.1111/1758-2229.13159> This is an open access article under the terms of the Creative Commons Attribution License, which permits use, distribution and reproduction in any medium, provided the original work is properly cited. ©2023 The Authors. Environmental Microbiology Reports published by Applied Microbiology International and John Wiley & Sons Ltd. Environmental Microbiology Reports. 2023; 1–18. wileyonlinelibrary.com/journal/emi41

The output can be accessed at:

<https://repository.rothamsted.ac.uk/item/989x3/abundance-and-phylogenetic-distribution-of-eight-key-enzymes-of-the-phosphorus-biogeochemical-cycle-in-grassland-soils>.

© 10 May 2023, Please contact library@rothamsted.ac.uk for copyright queries.

Abundance and phylogenetic distribution of eight key enzymes of the phosphorus biogeochemical cycle in grassland soils.

Journal:	<i>Environmental Microbiology</i>
Manuscript ID	Draft
Wiley - Manuscript type:	Research Article
Date Submitted by the Author:	n/a
Complete List of Authors:	Garaycochea, Silvia; National Institute of Agricultural Research Experimental Station Wilson Ferreira Aldunate, Biotechnology Unit Altier, Nora; National Institute of Agricultural Research Experimental Station Wilson Ferreira Aldunate Leoni, Carolina; National Institute of Agricultural Research Experimental Station Wilson Ferreira Aldunate Neal, Andrew; Rothamsted at North Wyke Romero, Héctor; University of the Republic Faculty of Sciences, Laboratorio de Organización y Evolución del Genoma/Genómica Evolutiva, Departamento de Ecología y Evolución,; University of the Republic Faculty of Sciences, Laboratorio de Organización y Evolución del Genoma/Genómica Evolutiva, Departamento de Ecología y Evolución,
Keywords:	functional diversity, metagenomics/community genomics, soil microbes, microbiome
Abstract:	Grasslands are one of the most diverse and widely distributed biomes on the Earth's surface. Nutrient cycling is one of the main ecosystem services provided by grasslands. The organic fraction of phosphorus (P) represents over half of the total P in soil and is a valuable reservoir. Soil microorganisms, involved in the P cycle, mediate organic P release through three enzyme families: alkaline phosphatases, nonspecific acid phosphatases, and phytases (P-enzymes). This study aimed, through a metagenomic approach, to assess the abundance and phylogenetic distribution of prokaryotic P-enzymes in a wide distribution of grass biomes across the globe and how they are related with environmental variables. To generate a functional perspective of phosphorus cycling, 74 soil metagenomes from 17 sites/projects representing different environmental conditions were examined for eight key P-enzymes. Multivariate analyses showed that Tmax, pH and evapotranspiration were highly associated with P-enzymes abundance and diversity. In addition, they tend to respond in a correlated manner to these variables suggesting an intricate relationship of abundance and diversity between them. On the other hand, their association with the general functional profiles was more idiosyncratic.

1
2
3
4
5
6
7
8
9
10
11
12
13
14
15
16
17
18
19
20
21
22
23
24
25
26
27
28
29
30
31
32
33
34
35
36
37
38
39
40
41
42
43
44
45
46
47
48
49
50
51
52
53
54
55
56
57
58
59
60



SCHOLARONE™
Manuscripts

1
2 1 Title: Abundance and phylogenetic distribution of eight key enzymes of the phosphorus biogeochemical cycle in grassland
3
4 2 soils.

5
6 3
7
8 4 Running title: Prokaryotic P - enzymes in grassland soil.

9
10 5
11 6
12
13 7 Authors: Garaycochea S.*¹, Altier N.¹, Leoni C.¹, Andrew L. Neal³, Romero H.*²

14
15
16 8 ¹ Instituto Nacional de Investigación Agropecuaria (INIA), Estación Experimental INIA Las Brujas, Ruta 48 Km 10,
17
18 9 Canelones, 90200, Uruguay.

19
20 10 ² Laboratorio de Organización y Evolución del Genoma/Genómica Evolutiva, Departamento de Ecología y Evolución,
21
22 11 Facultad de Ciencias/CURE, Universidad de la República, Maldonado, Uruguay

23
24 12 ³Net-Zero and Resilient Farming, Rothamsted Research, North Wyke, Okehampton, EX20 2SB, UK.

25
26 13 corresponding authors: Héctor Romero – elelor@fcien.edu.uy; Silvia Garaycochea – sgaraycochea@inia.org.uy

27
28 14
29
30 15
31
32 16 Silvia Garaycochea – sgaraycochea@inia.org.uy. Orcid: <https://orcid.org/0000-0001-9685-0584>

33
34 17 Nora Altier – naltier@inia.org.uy. Orcid: <http://orcid.org/0000-0002-3173-6016>

35
36 18 Carolina Leoni – cleoni@inia.org.uy. Orcid: <http://orcid.org/0000-0002-3891-564X>

37
38 19 Andrew L. Neal – andy.neal@rothamsted.ac.uk. Orcid: <http://orcid.org/0000-0003-4225-1396>

39
40 20 Héctor Romero – elelor@fcien.edu.uy. Orcid: <https://orcid.org/0000-0001-9685-0584>

41
42 21
43
44 22 All data used in this work are publicly available

45
46 23 This work was funded by the Instituto Nacional de Investigación Agropecuaria, INIA (Project SA47, SA 26 and SA 24),
47
48 24 Agencia Nacional de Investigación e Innovación (POS NAC 2015 1 110075).

49
50 25 Conflict of interest. None declared.

51 26

52
53 27

54
55 28

56
57 29

58

59

60

1
2 30 Abstract:
3

4 31
5

6 32 Grasslands are one of the most diverse and widely distributed biomes on the Earth's surface. Nutrient cycling is one of the
7
8 33 main ecosystem services provided by grasslands. The organic fraction of phosphorus (P) represents over half of the total P
9
10 34 in soil and is a valuable reservoir. Soil microorganisms, involved in the P cycle, mediate organic P release through three
11
12 35 enzyme families: alkaline phosphatases, nonspecific acid phosphatases, and phytases (P-enzymes). This study aimed,
13
14 36 through a metagenomic approach, to assess the abundance and phylogenetic distribution of prokaryotic P-enzymes in a wide
15
16 37 distribution of grass biomes across the globe and how they are related with environmental variables. To generate a
17
18 38 functional perspective of phosphorus cycling, 74 soil metagenomes from 17 sites/projects representing different
19
20 39 environmental conditions were examined for eight key P-enzymes. Multivariate analyses showed that Tmax, pH and
21
22 40 evapotranspiration were highly associated with P-enzymes abundance and diversity. In addition, they tend to respond in a
23
24 41 correlated manner to these variables suggesting an intricate relationship of abundance and diversity between them. On the
25
26 42 other hand, their association with the general functional profiles was more idiosyncratic.
27

28 43

29
30 44 **Keywords:** alkaline phosphatases, acid phosphatases, phytases, grasslands, phosphorus cycle
31

32 45
33

34 46
35

36 47
37

38 48
39

40 49
41

42 50
43
44
45
46
47
48
49
50
51
52
53
54
55
56
57
58
59
60

51 Introduction

52

53 Grasslands are one of the most numerous and widely distributed biomes on the Earth's surface. Factors defining grassland
54 biomes are climatic conditions, grazing and fire (White et al., 2000; Zhou et al., 2017). They develop in arid and semi-arid
55 areas, with seasonal cold and dry periods, and high rates of evapotranspiration (Knapp et al., 2002; Lenhart et al., 2015;
56 Barnet and Facey, 2016). The plant community is dominated by grasses and grass-like species, as well as other shrubby
57 species with different lifestyles. Plant community assemblages depend largely on climatic variables. Most grassland
58 biomass is above-ground: this, as well as the low rates of decomposition, generates significant accumulations of organic
59 matter in grassland soils (Blair et al., 2014). Grasslands provide several key ecosystem services, such as food, fiber and
60 forage production, water and nutrient cycling, and erosion control. Grassland biomes are habitat for a high diversity of
61 plants, animals and microorganisms (Le Roux et al., 2011; Blair et al., 2014).

62

63 Nutrient cycling, one of the main ecosystem services provided by grasslands, can be defined as the cycling of elements
64 carbon (C), nitrogen (N), and phosphorus (P) between different pools (Dubeux et al., 2007). The principal C pool is soil
65 organic matter, related to the type of vegetation and the amount of biomass below-ground. The availability of and cycling of
66 the three nutrients are connected. N addition is known to influence multiple ecosystem functions (Li et al., 2015), including
67 plant productivity, nutrient pools, organic matter decomposition and soil carbon stocks. Moreover, excessive N fertilization
68 leads to an imbalance of N and P availability (Elser et al. 2009; Peñuelas et al. 2013; Cui et al., 2022). Soil P is present as
69 two fractions, organic and inorganic phosphates. Low levels of soluble forms of P result from the high reactivity of both
70 fractions with calcium (Ca), iron (Fe) or aluminum (Al) ions present in soil, forming complex insoluble associations (Achat
71 et al, 2016).

72

73 The proportion of each P fraction varies between soils, dependent mainly upon the parent material, pH, temperature and
74 organic matter inputs (Zhou et al., 2017; Gaiero et al., 2020). The organic fraction accounts for over half of total soil P and
75 is a valuable reservoir that could be potentially mobilized (Condrón et al., 2005; Haygarth et al., 2013; George et al., 2018).
76 The organic P forms more abundant in soils are inositol phosphate, phospholipids, and nucleic acids (Gyaneshwar et al.,
77 2002). Inositol phosphate (commonly called phytic acid) can account for up to 80% or more of total organic P
78 (Quiquampoix and Mousain, 2005; Gerke, 2015). Phytic acid reacts with ions present in the soil forming stable and

79 insoluble complexes and so tends to accumulate in natural grasslands soils. Phospholipids and nucleic acids are both labile
80 and readily accessible to soil organisms (Gerke, 2015).

81
82 Soil microorganisms are an integral part of the soil P cycle, mediating P release for plants (Awasthi et al., 2011; Richardson
83 and Simpson, 2011). Mineralization of organic P by microbes is strongly influenced by environmental variables (Seshachala
84 and Tallapragada, 2012; Alori et al., 2017). Release of phosphate from organic P is mediated by three broad groups of
85 enzymes: 1) alkaline phosphatases that catalyze the hydrolysis between the carbon and phosphorus in organic phosphates
86 esters, 2) non-specific acid phosphatases, which perform the desphosphorylation of phospho-ester bonds or
87 phosphoanhydride in organic matter and 3) phytases, which specifically cause the release of P from phytic acid (Rossolini et
88 al., 1998; Huang et al., 2009; Jorquera et al., 2008; Bergkemper et al., 2016; Morrison et al., 2016; Gaiero et al., 2020).

89 Alkaline phosphatases are produced by a broad range of bacteria, archaea and fungi and are considered the most important
90 in the microbial P turnover (Li et al., 2021). They are grouped in three families, PhoA, PhoD and PhoX, with PhoD the most
91 abundant and ubiquitous (Ragot et al, 2015). Both PhoD and PhoX were identified as Ca²⁺-dependent extracellular enzymes
92 and PhoA as a Zn²⁺-dependent intracellular enzyme (Neal et al., 2018). All are regulated by P availability under control of
93 the Pho regulon (Santos-Beneit et al., 2015; Li et al., 2021). Alkaline phosphatases show a broad substrate specificity and
94 high catalytic efficiency (Rodriguez et al., 2014; Cai et al., 2021). These characteristics enable microorganisms harboring
95 these genes to use alternative P sources under P-limited conditions, conferring them an advantage over the plants (Li et al.,
96 2021).

97
98 Acid phosphatases are another group of enzymes distributed widely among microorganisms and plants. They are divided
99 into three families, Nsap class A, Nsap class B and Nsap class C, none of them exhibit strong substrate specificity, hence
100 their names (Thaller et al., 1998). These enzymes are mostly produced by microorganisms and are mostly active in acid
101 soils (Gaiero et al., 2018). Until now, the mechanisms involved in catalytic activity and its regulation are not well
102 understood. To expand the knowledge of these enzymes, metagenomic studies have been carried out to understand how they
103 vary in abundance and diversity in different environments (Bergkemper et al., 2016; Neal et al., 2018). Neal et al. (2018)
104 showed that Nsap class C, a putative extracellular enzyme, was predominant in acid soils under P limiting conditions
105 compared to Nsap class A, an intracellular enzyme mainly produced by plants and rhizosphere microorganisms. There is no
106 evidence that non-specific acid phosphatases are regulated by the Pho regulon.

107

1
2 108 Phytases are produced by bacteria, fungi, plants and animals able to catalyze mineralization of organic P from phytate to
3
4 109 inorganic P (Jorquera et al., 2008; Tu et al., 2011; Ariza et al., 2013). Phytase families more common in microorganisms are
5
6 110 the beta-propeller phytase (BPP), protein tyrosine phosphatase-like cysteine phytase (CPhy) and histidine acid phytase
7
8 111 (HAPhy) (Lim et al., 2007). The main differences between the phytase families are structural, mainly related to differences
9
10 112 in the active site which determines which phosphate group of the phytate is dephosphorylated, and co-factor requirements.
11
12 113 Despite this, all phytases can release the six phosphate molecules contained in phytate (Misset, 2002). The phytase enzymes
13
14 114 are distributed throughout soils, but the higher concentrations are found in the rhizosphere (Li et al., 2008). Phytases exhibit
15
16 115 different pH and temperature optima in the laboratory (Caffaro et al., 2020). Moreover, enzymatic activity is affected by soil
17
18 116 type, texture and mineralogy by varying the ability to retain an active enzyme (Rao et al., 1994; Tang et al., 2006; Azeem et
19
20 117 al., 2014)

21 118
22
23 119 The P cycle is determined by different environmental variables such as plant community, organic matter content, soil
24
25 120 properties and climatic conditions. Knowledge about the key microbial enzymes involved in organic P mineralization is
26
27 121 different to each class of enzymes. This study aimed, through a metagenomic approach, to assess for the first time how key
28
29 122 P cycling enzymes vary in their abundance and diversity and how this is related with environmental variables in the
30
31 123 grassland biome on a global scale. Grasslands, one of the five most important biomes on earth due to the biodiversity it
32
33 124 harbors and its economic importance, makes it necessary to have a deeper understanding of its functions and dynamics for
34
35 125 its preservation.

36 126 37 38 127 39 40 128 Experimental Procedures

41 42 129 43 44 130 Data collection

45
46 131 A total of 376 geo-referenced metagenomes samples from 17 projects deposited with MG-RAST were selected through the
47
48 132 TerrestrialMetagenomeDB (<https://webapp.ufz.de/tmdb/>) applying the following filters: Source DB: MG-RAST;
49
50 133 seq_technology: Illumina; material: soil; Biome: grasslands, temperate grasslands, savanna and shrubland to assembly the
51
52 134 grassland soil metagenomes samples set. The set of environmental variables was assembled, including soil properties and
53
54 135 climatic variables for each sample based on its geographic location. Soil type and physicochemical properties were
55
56 136 obtained from SoilGrid 250m 2.0 – ISRIC World Soil Information. The following properties were included Bulk Density

1
2 137 (BD; cg cm^{-3}), Clay (g kg^{-1}), Sand (g kg^{-1}), Silt (g kg^{-1}), Cation Exchange Capacity at pH 7 (CEC; mmol(c) kg^{-1}), Total
3
4 138 Nitrogen (N; cg kg^{-1}), Soil Organic Carbon (SOC; cg kg^{-1}), pH (water*10). The organic available P (Pav) was estimated
5
6 139 based on SOC and N content following a model proposed by Tian et al. (2010). The climate variables were obtained from
7
8 140 TerraClimate (<https://www.climatologylab.org/terraclimate.html>), including maximum temperature, (T_{max} ; $^{\circ}\text{C}$),
9
10 141 Precipitation, (ppt; mm), actual evapotranspiration (aet; mm), soil moisture (moisture; mm) and runoff (q; mm) (Table S1).
11
12 142 Hereafter they are called environmental variables. The collinearity analysis on the environmental variables set was
13
14 143 performed with R-base (R core Team 2022). The variables included in the set were those with $r \leq 0.5$ and meaningful to
15
16 144 the study.

17 145
18
19 146
20
21 147 The soil metagenome sequencing from projects mgp91922 and mgp93346 (Uruguay) were carried out on a HiSeq Illumina
22
23 148 platform, (Service CD Genomics, NY, USA; pair-end read 150 bp). Raw sequence quality was analyzed with FastQC
24
25 149 software version 0.11.2. Assembly and functional annotation was performed on the MG-RAST repository. Raw sequence
26
27 150 data are publicly available on the MG-RAST repository.

28
29 151 The functional annotation based on MG-RAST subsystems level 2 of the 376 selected metagenomes was obtained from
30
31 152 MG-RAST repository (Meyer et al. 2008).

32 153 The set of predicted proteins to each metagenome was obtained through the RESTful API of MG-RAST (Wilke et al.,
33
34 154 2015). Protein sequences were downloaded using a matR version 0.9.1 package R (Braithwaite et al., 2018).

35
36 155
37
38
39 156 Statistical analyses

40 157
41
42 158 Uniform Manifold Approximation and Projection version 3 (UMAP, McInnes et al., 2018) was used to explore the
43
44 159 variability of metagenome functional profiles (subsystems level 2) implemented in the umap R package using default
45
46 160 parameters. Data normalization was done with the Variance Stabilizing Transformation (VST) method implemented in
47
48 161 DESeq2 R package (Love et al., 2014) with a nonspecific model.

49
50 162 Canonical analysis of principal coordinates (CAP) (Anderson and Willis 2003) implemented in Vegan R Package version
51
52 163 2.6.2 (Oksanen et al., 2019) was performed based upon Mahalanobis distance to calculate the relationship between the
53
54 164 metagenomes functional profiles (subsystems level 2) and environmental variables. Significance of the model parameters
55
56 165 was determined with permutational multivariate analysis of variance (ANOVA) with 999 permutations.

57
58
59
60

1
 2 166 Hereafter, all analyses were performed on a reduced samples subset, in order to minimize the bias generated by the different
 3
 4 167 number of samples in each MG-RAST project. This subset included a maximum of 3 samples per MG-RAST project with
 5
 6 168 the same geo-reference. Finally, the reduced subset was made up of 74 samples from the 17 MG-RAST projects (Table S3).
 7
 8 169
 9
 10 170 Protein/function count matrix (level 4 in the MG-RAST nomenclature), including the 8 P-enzymes, for the 74 selected
 11
 12 171 metagenomes was normalized with CPM and TMM methods using the edgeR package (doi:
 13
 14 172 10.1093/bioinformatics/btp616). This data was used to perform the direct correlations of P-enzymes with environmental
 15
 16 173 variables.
 17
 18 174

19 175 The reference databases of the phosphatases and phytases (from now called P-enzyme) used in this work were built by Neal
 20
 21 176 et al., (2017). The P-enzymes included are listed in Table 1.
 22
 23 177
 24 178

25 **Table 1:** List of P-enzymes included in the analyses.
 26

Enzyme	Gene	Predicted Cellular Localization	Number of protein sequences in reference database
PhoA	<i>phoA</i>	Periplasmic/Cytoplasmic	293
PhoD	<i>phoD</i>	Outer membrane/extracellular	833
PhoX	<i>phoX</i>	Outer membrane/extracellular	424
Nsap class A (Nsap-A)	<i>phoC</i>	Periplasmic/Cytoplasmic	750
Nsap class B (Nsap-B)	<i>aphA</i>	Periplasmic/Cytoplasmic	388
Nsap class C (Nsap-C)	<i>olpA</i>	Outer membrane/extracellular	1123
β -propeller phytase (BPP)	<i>phyL, phyS</i>	Outer membrane/extracellular	108
Cysteine phytase (Cphy)	<i>phyA</i>	Outer membrane/extracellular	122

extracellular

179

180

181 Protein sequence alignments of the respective reference database was performed using MAFFT version 7.4.60 (Katoh et al.,
182 2002) under default parameters. Reference protein phylograms were visualized with IQTree 2 version 1.6.12 (Minh et al.,
183 2020) and the evolutionary models were evaluated with RAxML-NG (Kozlov et al., 2019). Phylograms were plotted with
184 iTOL (Interactive Tree of Life; Letunic and Bork 2007).

185 To determine the abundance and diversity of the P-enzymes in the metagenomes, the predicted protein sets were aligned
186 with each P-enzyme reference database. First, the whole protein set was aligned against each P-enzyme reference database
187 using HMMER version 3.3.1 (hmmer.org). Then, the sequences with positive hits were extracted using the esl-fetch tool.
188 Finally, these sequences were aligned to the correspondent reference database using MAFFT with default parameters.
189 Maximum likelihood-based phylogenetic placement of metagenome-derived protein sequences on the appropriate P-enzyme
190 reference phylogram was performed with EPA-ng (Barbera et al., 2019). Edge-PCA ordination and Kantorovich-Rubinstein
191 (KR) distance metrics (Evans and Matsen, 2012; Matsen and Evans, 2013) were computed on these results. The edge-PCA
192 and KR distances were performed using gappa (Czech et al., 2020) and tree and domain composition diagrams were drawn
193 using Archaeopteryx (<https://sites.google.com/site/cmzmasek/home/software/forester>).

194

195 Canonical analysis of principal coordinates (CAP) (Anderson and Willis 2003) implemented in the Vegan R Package
196 version 2.6.2 (Oksanen et al., 2019) was used to evaluate the relationship between the abundance and diversity of P specific
197 functions with the environmental variables. A CAP analysis associating enzyme abundance with environmental variables
198 was performed using Mahalanobis distance. Each enzyme abundance in each sample was normalized in relation to the
199 sequencing coverage of each enzyme. Significance of the model parameters was determined with permutational multivariate
200 analysis of variance (PERMANOVA) with 999 permutations. The KR distance of each enzyme calculated as mentioned
201 above was used to perform the CAP analyses between abundance and diversity of each P-enzyme and environmental
202 variables. Significance of the model parameters was determined with PERMANOVA based upon 999 permutations.
203 Graphics were produced with the R package ggplot2 (Wickham, 2016). All basic statistical procedures were performed
204 using R-base (R core Team 2022).

205

206

207 Results

208

209 To generate a general perspective of grassland functional landscapes, an analysis was performed on a set of 376 grassland
210 soil metagenomes. Based upon the distribution of 168 functional process or subsystem MG-RAST annotations (Table S1
211 and S2) we identified a strong association of clusters with geographic location/project and soil type: Kastazoem/Luvisol,
212 Luvisol/Kastazoem, Fluvisol, Kastazoem (Fig. S1) based upon Uniform manifold approximation and projection (UMAP)
213 analysis (McInnes et al., 2020). Besides this, samples from two different projects with soil classified as Phaeozem, were
214 grouped together with Andosols. Two small groups of samples with soils classified as Kastazoem/Luvisol and Fluvisol were
215 not clustered with soil samples with the same classification. Only one cluster was formed of samples from different projects
216 and soil classifications. Within this cluster, a separation among samples was observed, mainly due to environmental
217 variables. Samples from Brazil (Ferrasols), Uruguay (Vertisol/Phaeozem, Molisols/Phaeozem), and England (Cambisols),
218 with high maximum temperatures (T_{\max}) and soil moisture, and low pH clustered together. Samples from the USA
219 (Chernozem and some Kastazoem) with low T_{\max} , soil moisture and neutral pH form another cluster and two subgroups
220 related to different soil types were also observed (Fig. S1). Subsequent analyses were performed on a balanced reduced
221 subset of 74 grasslands soil metagenomes to minimize any bias associated with including different numbers of samples
222 within each project (see methods and Table S3).

224 *Metagenome subsystem profiles and environmental variables.*

225 Canonical Analysis of Principal Coordinates (CAP) was performed to explore the relationship between environmental
226 variables (Table S3) and soil microbial functional profiles (MG-RAST level 2 subsystem annotations, Table S4). The
227 constrained model was significant ($p = 0.001$) and explained 24.8% of total variance observed in the data set. Significant
228 associations ($r > |0.20|$, $p < 0.01$) between the distribution of metagenomes and nine environmental variables were
229 identified. CAP1 axis was correlated with pH ($r = -0.743$), bulk density (BD, $r = -0.521$), soil organic carbon (SOC, $r =$
230 0.564), and moisture ($r = 0.536$). This axis separated samples from low pH soils (e.g.: mgp9904, mgp5588, mgp91922 and
231 mgp93346) from those with neutral pH (mgp13948 among others). CAP2 axis was associated principally with pH ($r = -$
232 0.486), SOC ($r = -0.220$), and T_{\max} ($r = 0.664$), runoff (q, $r = 0.490$), moisture ($r = 0.476$) and Clay ($r = 0.231$). Extreme
233 values of the CAP2 axis corresponded to mgp10450 and mgp10451 (both from Brazil) which were associated with the
234 highest T_{\max} , moisture and ppt values of the set (Table 2, Table S5, Fig. S2).

1
2 235
3
4 236 *Analyses based on abundance of P-enzymes genes.*
5
6
7 237 Each metagenome predicted protein set was interrogated against of their correspondent reference database of the PhoD,
8
9 238 PhoX, PhoA, Nsap-A, Nsap-B, Nsap-C, BPP and CPhy enzymes to obtain the abundance and phylogenetic distribution of
10
11 239 P-enzyme coding genes. Inferred protein abundances in each soil metagenome is shown in Table S6 and phylogenetic
12
13 240 placements in Figure 1 and Figure S3.
14
15 241 The enzymes with highest relative abundance in global grasslands were alkaline phosphatases PhoD and PhoX (Table S6)
16
17 242 both having broad phylogenetic distributions and no clear dominant phylotypes (Fig. 1a and Fig. 1b). PhoA had a median of
18
19 243 23.3 hits with a limited phylogenetic distribution (Fig. S3, Table S6).
20
21 244 Nsap-A and Nsap-C were the most abundant acid phosphatases and presented a different distribution in their corresponding
22
23 245 phylogenetic trees. Whilst Nsap-A showed a broad distribution within its phylogeny (Fig. 1c), Nsap-C was linked to main
24
25 246 branches of alpha and gammaproteobacteria, Flavobacteria, and Sphingobacteria classes. On the other side, Nsap-B had a
26
27 247 low abundance and only gammaproteobacteria variants were found.
28
29 248 BPP was the most abundant phytase with a phylogenetic distribution mainly restricted to the Proteobacteria phylum (e.g.:
30
31 249 *Pseudomonas*, *Alteromonas*, *Acinetobacter*) (Fig. 1d, Table S6). The CPhy phytase, with lower abundance, is distributed
32
33 250 within Betaproteobacteria, Gammaproteobacteria and some classes of the Firmicutes phylum (Fig. S3, Table S6).
34
35 251
36
37 252 **Figure 1:** Phylogenetic placements of the predicted proteins of each metagenome with respect to the reference bases of
38
39 253 each enzyme: a) PhoD, b) PhoX, c) Nsap-A and d) BPP The size of the circle representing placements is proportional to the
40
41 254 abundance. Maximum likelihood-based phylogenetic placement of metagenome-derived protein sequences was performed
42
43 255 with EPA-ng and tree drawn with iTOL. The circle sizes represent the number of hits per node.
44
45 256
46
47 257 Correlation analyses between normalized enzyme abundance (by CPM and TMM methods) and environmental variables
48
49 258 showed that PhoD, PhoX and BPP had a significant correlation with the pH, actual evapotranspiration (aet), precipitation
50
51 259 (ppt), runoff (q) and soil moisture. In addition, PhoD showed significant correlation with SOC and Pav. NsapC showed
52
53 260 significant correlation with aet, q, ppt and moisture (Table S7).
54
55 261
56
57 262 We used CAP analysis to explore the relationship between total enzyme abundance and environmental variables (Fig. S4).
58
59 263 The constrained model based on Mahalanobis distance explained 36.4% of variance within the data set ($p = 0.001$). The
60

1
2 264 alkaline phosphatases PhoD, PhoX and PhoA were mainly associated with the explained variance. CAP1 axis explained
3
4 265 8.9% of variance ($p = 0.001$) and was associated with pH ($r = -0.70$), BD ($r = -0.48$), Sand content ($r = -0.40$), ppt ($r =$
5
6 266 0.74), aet ($r = 0.67$), SOC ($r = 0.52$), Pav ($r = 0.52$) and Silt ($r = 0.49$). Samples from metagenomes of clay soils with low
7
8 267 pH (5.0 to 6.8) and high SOC values (Androsols, Cambisols, Ferrasols, Fluvisols, Kastanozem/Luvisol,
9
10 268 Luvisol/Kastanozem) were separated in this axis from those of neutral or alkaline soils having lower SOC contents
11
12 269 (Chernozem, Luvisol and Kastanozem). CAP2 axis was associated with T_{\max} ($r = -0.40$), BD ($r = -0.34$), pH ($r = -0.27$), ppt
13
14 270 ($r = 0.41$), actual evapotranspiration (aet, $r = 0.39$) and q ($r = 0.39$). Soil metagenomes associated with lower aet values and
15
16 271 relatively high T_{\max} were separated on this axis. All variables were significant with a $p < 0.001$ (Table 2 and Table S8).
17
18 272

19 273 *Analyses based on the abundance and phylogeny of P-enzyme genes*

20
21 274 To gain deeper insight in the diversity and abundance of P-enzymes, CAP analyses were performed using Kantorovich –
22
23 275 Rubinstein (KR-CAP) distance matrices between samples to include not only abundance but also phylogenetic information.
24
25 276 PhoD KR-CAP analysis explained 49.8% of the total variance in the data set ($p < 0.001$). Eleven of the environmental
26
27 277 variables were associated with the first two KR-CAP axes. The KR-CAP1 axis was associated negatively with pH ($r = -$
28
29 278 0.75), BD ($r = -0.39$), Sand ($r = -0.28$), CEC ($r = -0.22$) and positively with ppt ($r = 0.80$), aet ($r = 0.79$), q ($r = 0.72$), Tmax
30
31 279 ($r = 0.313$), Silt ($r = 0.27$) and SOC ($r = 0.22$). This axis separated soils with low pH, relative high values of SOC and Tmax
32
33 280 (Cambisols, Ferrasols, Mollisols/Phazoem, Luvisol/Kastanozem) to the soils with higher pH and lower Tmax. The KR-
34
35 281 CAP2 axis was characterized by a negative association with T_{\max} ($r = -0.41$), moisture ($r = -0.29$) and Silt ($r = -0.22$). This
36
37 282 axis separated soil with neutral pH and relatively high Silt and Sand values from the rest samples (Table S9, Figure 2).
38
39 283

40 284 **Figure 2:** CAP based on Kantorovich-Rubinstein distance for PhoD. PERMANOVA analysis with 999 permutations was
41
42 285 performed to determine the significance between the sites/MG-RAST project. For each MG-RAST project three samples
43
44 286 with the same geo-reference were included. Each point represents samples from the project mpg1992 (blue); mpg3520
45
46 287 (green); mpg5588 (dark red); mpg7792 (grey); mpg8624 (mustard); mpg9904 (violet); mpg10450 (dark blue); mpg10523
47
48 288 (stone blue); mpg10541 (turquoise); mpg10956 (yellow); mpg13011 (lilac); mpg13520 (jade); mpg13948(orange);
49
50 289 mpg20922 (brown); mpg89409 (brick-red); mpg91922. (light green); mpg93346 (light blue). Vector lengths represent the
51
52 290 correlation between each variable and the axes. CAP analysis was performed with the Vegan R package and graphics were
53
54 291 produced with the R package ggplot2.
55
56 292

1
2 293 The same analysis was performed for the other enzymes and the results are summarized in Table 2 (Tables S10 to S16, Fig.
3
4 294 S5 to S7). Notably, pH, T_{\max} and aet were associated with all enzyme distributions. SOC displayed a high relationship with
5
6 295 alkaline phosphatases PhoD and PhoX, and acid phosphatases Nsap-A and Nsap-C and estimated phosphorus (Pav) was
7
8 296 mainly associated with the phytases. Next, CEC showed a high correlation with alkaline phosphatases and phytases. Finally,
9
10 297 clay content was related mainly to alkaline phosphatases (Table 2).

11 298
12
13 299 **Table 2:** Canonical Correlation Analysis (CAP) summaries. CAP analyses based on Mahalanobis distance for MG-RAST
14
15 300 level 2 subsystem annotations and enzyme abundance and based on Kantorovich-Rubinstein distance for each of eight
16
17 301 enzymes. Environmental variables included: pH, Soil Organic Carbon (SOC), Phosphorous estimated (Pav), Cation
18
19 302 Exchange Capacity (CEC), Bulk Density (BD), Clay, Sand, silt, actual evapotranspiration (aet), runoff (q), soil moisture
20
21 303 (moisture), precipitation (ppt), maximum Temperature (T_{\max}). PERMANOVA analysis with 999 permutations was
22
23 304 performed to determine the significance between the sites/MG-RAST project. The values marked with red are significant.

305 306 307 308 *Covariation of P-enzymes genes*

309 In order to examine the co-variation between P-enzymes their KR-CAP analyses results were compared. First, the enzymes
310 were grouped in alkaline phosphatases (PhoD, PhoX and PhoA), acid phosphatases (NspA-to-C) and phytases (BPP and
311 Cphy), then a simple within group analysis was carried out by correlating their KR-CAP axes. For the case of the alkaline
312 phosphatases PhoD and PhoX there was a strong positive correlation between KR-CAP2 PhoD and KR-CAP1 PhoX ($r =$
313 0.87). Both PhoA KR-CAP axes showed significant correlations with KR-CAP2 PhoD ($r = 0.41$, $r = 0.51$, respectively) and
314 KR-CAP1 PhoX ($r = 0.46$ and $r = 0.44$, respectively) (Figure 3a, Table S17).

315 The acid phosphatases Nsap-A and Nsap-C KR-CAP axes were highly correlated ($r = 0.78$ for KR-CAP1s and $r = 0.49$ for
316 KR-CAP2). Moreover, both showed significant, albeit lower, correlations with Nsap-B (Figure 3b, Table S17).

317 Related to the phytases, the correlation analysis between KR-CAP axes of BPP and Cphy showed a significant and high
318 correlation between their CAP axes (Figure 3c, Table S17).

1
2 319 When comparing the most abundant enzymes between groups, a significant and high positive correlation among both
3
4 320 alkaline phosphatases PhoD and PhoX with the acid phosphatases Nsap-A and Nsap-C, was observed (Figure 3d, Table
5
6 321 S17)

7
8 322 Finally, when comparing each P-enzyme CAP analysis with the subsystem level CAP-analysis we observed that only PhoD
9
10 323 (CAP1-PhoD vs CAP2-SS = 0.44), BPP(CAP1-BPP vs CAP1-SS = -0.41, CAP2-BPP vs CAP2-SS = 0.55) and CPhy
11
12 324 (CAP1-Cphy vs CAP1-SS = -0.59), displayed significant correlations between the axes (Table S18).
13
14

15 325

17 326 **Figure 3:** Correlation matrix of KR-CAP axes. a) Correlogram of the alkaline phosphatases displays the Pearson correlation
18
19 327 coefficients between KR-CAP PhoD axes, KR-CAP PhoX and KR-CAP PhoA; KR-CAP PhoX and KR-CAP PhoA. The
20
21 328 correlation coefficients are colored according to their values; being blue the positive values and red the negative values. b)
22
23 329 Correlogram of the acid phosphatases displays the Pearson correlation coefficients between KR-CAP Nsap-A axes, KR-
24
25 330 CAP Nsap-B and KR-CAP Nsap-C; KR-CAP Nsap-B and KR-CAP Nsap-C. The correlation coefficients are colored
26
27 331 according to their values; being blue the positive values and red the negative values. c) Correlogram of the phytases
28
29 332 displays the Pearson correlation coefficients between KR-CAP BPP axes and KR-CAP CPhy. The correlation coefficients
30
31 333 are colored according to their values; being blue the positive values and red the negative values. d) Correlogram of the
32
33 334 most abundance displays the Pearson correlation coefficients. The correlation coefficients are colored according to their
34
35 335 values; being blue the positive values and red the negative values. Correlation analysis and graphics were performed with
36
37 336 cor R package.
38
39 337

41 338 *Edge-PCA and taxonomic identification of differentially observed P-enzymes*

42
43
44 339 Edge-PCA analysis was applied to reveal the differential presence and abundance of P-enzyme variants among the soil
45
46 340 metagenomes; a summary of the results is shown in Table S19. Variability in the abundance of PhoD variants associated
47
48 341 with the first edge-PCA axis separated samples by soil type, pH and SOC content. The differences showed that the enzyme
49
50 342 variants of the species *Koribacter versatilis* (class Acidobacteria) and *Rhodanobacter spathiphylli* (class
51
52 343 Gammaproteobacteria) (Figure 4b) were more abundant in soils classified as Ferrasols, Cambisols, Molisols/Phaeozem and
53
54 344 Vertisol/Phaeozem with low pH and relatively high SOC content (left quadrant of Figure 4a and). Enzyme variants
55
56 345 associated with *Actinomyces*, *Bacillus* and *Planctomyces* (Figure 4b) were more abundant in Kastanozem, Chernozem,
57
58
59
60

1
2 346 Luvisol and Fluvisols soils with higher pH and lower SOC content (right quadrant of Figure 4a). The second axis was
3
4 347 associated with PhoD genes harbored by *Burkholderia* and *Acinetobacter* with higher abundance in soils with neutral pH
5
6 348 and low clay content (Tables S1 and S19, Figure 4a).

7 349
8
9
10 350 **Figure 4:** a) Graphic representation of the first two axes of the edge-PCA for PhoD using samples as observations. Each
11 351 point represents samples from the project mpg1992 (blue); mpg3520 (green); mpg5588 (dark red); mpg7792 (gray);
12 352 mpg8624 (mustard); mgp9904 (violet); mgp10450 (dark blue); mgp10523 (stone blue); mgp10541 (turquoise); mgp10956
13 353 (yellow); mgp13011 (lilac); mgp13520 (jade); mpg13948(orange); mpg20922 (brown); mgp89409 (brick-red); mgp91922
14 354 (light green); mgp93346 (light blue). b) The phylogeny distribution of PhoD hits along the first and second axis of the
15 355 analysis (protein with positive coefficients are marked in blue and proteins with negative coefficients are marked in orange).
16 356 The edge-PCA was performed using gappa software and tree and domain composition diagrams were drawn using
17 357 Archaeopteryx (<https://sites.google.com/site/cmzmasek/home/software/forester>).

18
19
20
21
22
23
24
25 358
26
27 359 The alkaline phosphatases PhoX and PhoA showed a narrower phylogenetic distribution and Alphaproteobacteria (*Rosevivax*
28 360 and *Agrobacterium* among others) genes were predominant in soils with high SOC values and relatively low T_{max} (Table S1
29 361 and Table S19). The *Burkholderia* variants were observed in soil samples with near neutral pH and average SOC and CEC
30 362 values (Fig. S8). The genes PhoA of *Pantoea* and *Providencia* together with *Acinetobacter* and *Actinobacter* genera were
31 363 associated with varying abundance between samples (Fig. S8). Again, *Acinetobacter* was more abundant in soils with
32 364 *circum*-neutral pH and average SOC and CEC values (Fig. S8).

33
34
35
36 365 The acid phosphatases Nsap-A genes harbored by *Pedospaera*, *Dyella jiangningensis*, *Dyella japonica* and *Rhodanobacter*
37 366 sp. were identified as the most abundant among soils with average SOC and CEC values and sandy texture (Fig. S8). On the
38 367 other hand, *Sphingomonas* sp., *Phenylobacterium* sp., *Rhodanobacter* sp., and *Caulobacter* species variants were more
39 368 abundant in soils with high clay content (Fig. S8).

40
41
42
43
44 369
45
46
47 370 The Nsap-C genes harboring by *Stenotrophomonas* (gamma-Proteobacteria) and *Podospaera* were more abundant in soils
48 371 with low values of moisture and aet. *Enterobacter* Nsap-B variants predominated in soils classified as Ferrasols, Andosols
49 372 and Luvisol with acidic pH, low T_{max} , and high aet and ppt values. Metagenomes from Fluvisol, with a pH = 7, were
50 373 associated with a higher abundance of *Photobacter* and *Marinomonas* enzymes and were strikingly different to the rest
51 374 (Fig. S8).

1
2 375

3
4
5 376 BPP phytase genes were only found in soil samples with pH values above 6.6. BPP gene variants of the *Acinetobacter*,
6
7 377 *Pseudomonas*, *Methylophaga*, *Pseudoalteromonas* and *Alteromonadales* (Gammaproteobacteria), and *Shewanella* and
8
9 378 *Hylemonella* (Betaproteobacteria), were identified to dominate in clay soils with high CEC values. BPP genes harbored by
10
11 379 *Bacillus* species were most abundant in sandy soils with low nutrient content.

12 380

13
14 381 CPhy genes from *Bacillus*, *Acintebacter* and *Pseudomonas* genera varied across the samples but there was no clear signal
15
16 382 to reveal associations with environmental variables.

17
18
19
20
21
22
23
24
25
26
27
28
29
30
31
32
33
34
35
36
37
38
39
40
41
42
43
44
45
46
47
48
49
50
51
52
53
54
55
56
57
58
59
60

For Review Only

1
2 383 Discussion

3
4 384
5
6 385 The ecosystems are connections among different factors such as soil types, plant communities, microbial communities,
7
8 386 macro and micro fauna, climate conditions among others (Islam et al., 2020). The present work aimed to study the microbial
9
10 387 functional diversity of P-enzymes in the grassland biome, using a metagenomic approach. The analyzed samples represent
11
12 388 different environmental conditions defined by the physical and chemical soil properties, and climate variables (Amundson,
13
14 389 2013; Islam et al. 2020). The effect of specific plant communities was not considered in the analyses and could constitute a
15
16 390 limitant in the study.

17 391
18
19 392 The UMAP analysis showed sample clustering mainly based on the sampling sites/projects with the exception of a
20
21 393 heterogeneous group which was represented by samples from Latin America, United States and England. As expected, these
22
23 394 samples came from soils with differences in their geological origin, nutritional status, and water content. This group enabled
24
25 395 the study of the relation among environmental variables and functional microbial profiles using multivariate methods. In
26
27 396 accordance with different authors microbial functional profiles were associated to T_{max} (Johnston et al., 2019; Sorensen et
28
29 397 al., 2019), soil moisture (Bachar et al., 2010; Ochoa et al., 2010) and pH (Fierer and Jackson., 2006; Islam et al., 2020) and
30
31 398 to a lesser extent with SOC (Lauber et al. 2013), soil texture (Tecon and Or, 2017; Garaycochea, et al. 2020) and
32
33 399 evapotranspiration (aet). So far, there are no reports about the relation between evapotranspiration and microbial functional
34
35 400 profiles. These results reveal the complexity of the relation between microbial taxonomy and functional diversity and the
36
37 401 constraints for the understanding of which factors influence the community assembly and functions.

38 402
39
40 403 Microbial enzymes such as phosphatases (Rodríguez et al. 2006, Nannipieri et al. 2011) and phytases (Yao et al. 2012; Tan
41
42 404 et al., 2013) have a crucial role in phosphorus cycling. This study showed that the environmental variables T_{max} , pH, SOC
43
44 405 and soil moisture are associated with alkaline phosphatase abundance as mentioned by Gu et al. (2020) and Gaiero et al.
45
46 406 (2020). Microbial alkaline phosphatases (PhoD, PhoX and PhoA) are considered the most important enzymes for P cycling
47
48 407 (Sphon and Kuzyakov, 2013). The present work found that PhoD was the most abundant and had the widest phylogenetic
49
50 408 distribution regardless of the soil properties such as pH. Bergkemper et al. (2016) reported that the *phoD* genes were
51
52 409 identified as the most abundant even in acidic soils and demonstrated the importance of alkaline phosphatases in the
53
54 410 mineralization of soil organic P. In relation to gene abundance, PhoD was followed by PhoX and PhoA which showed a
55
56 411 lower abundance and narrower phylogenetic distribution. Ragot et al (2015) and Neal et al (2017) also reported that PhoD

1
2 412 was the most abundant alkaline phosphatase with a cosmopolitan distribution in marine and terrestrial systems. On the other
3
4 413 hand, PhoX was reported as mainly abundant in terrestrial ecosystems (Ragot et al., 2017). PhoA has only been studied by
5
6 414 Sebastian and Ammerman (2011) in a marine ecosystem.

7 415
8
9 416 PhoD and PhoX showed a high correlation with SOC and clay. There are several studies which demonstrate the effect of
10
11 417 SOC, N and organic P content on the abundance and diversity of both enzymes and the corresponding bacteria (Ragot et al.,
12
13 418 2017; Wei et al., 2021; Li et al., 2021). The predicted extracellular location of both enzymes (Neal et al., 2017) may explain
14
15 419 the importance of clay content in relation to the stabilization role due to the immobilization and the maintenance of the
16
17 420 enzymatic activity (Margalef et al., 2017). Even though PhoD is widely distributed among different classes of bacteria, in
18
19 421 this study, variants associated with *Koribacter versatilis* (Acidobacteria class) and *Rhodanobacter spathiphylli*
20
21 422 (Gammaproteobacteria class) were the most abundant in soils with relatively high SOC values and low pH. The *phoD*
22
23 423 associated with *Koribacter versatilis* has been identified as a dominant phylotype in a silty clay loam soil Chromic Luvisol in
24
25 424 the United Kingdom (Neal et al., 2017), and the *Rhodanobacter spathiphylli* associated phylotype has been identified as a
26
27 425 dominant phylotype in the rhizospheres of maize and sorghum in a Brazilian Distroferric Red Latosol (Neal et al., 2021).
28
29 426 Variants associated with *Actinomyces*, *Bacillus* and *Planctomyces* were prevalent in soils with lower SOC and neutral pH.
30
31 427 pH is the key variable explaining the difference in abundance of species since all reported species are heterotrophs (Kielak
32
33 428 et al., 2016; Saxena et al., 2020). Finally, the PhoX gene harbored by *Burkholderia* genus differed in soils with low and
34
35 429 medium content of SOC. Bacteria from this genus show a wide repertoire of metabolic pathways making them more
36
37 430 competitive in nutrient-restrictive environments (Morya et al., 2020).

38 431
39
40 432 Considering acid phosphatases, Nsap-A and Nsap-C were the most abundant and highly correlated with pH, T_{max} , aet, SOC
41
42 433 and Sand content. Nsap-A was found in *Dyella jiangningensis*, *Dyella japonica* and *Rhodanobacter* sp. These species use
43
44 434 different carbon sources and have been reported to be dominant in acid and neutral soils (Weon et al., 2009; Dahal et al.,
45
46 435 2017). On the other hand, Nsap-C was identified in Alpha and Gammaproteobacteria, Flavobacteria, and Sphingobacteria
47
48 436 classes, consistent with previous evidence (Neal et al., 2017; Gaiero et al., 2020). Contrary to the finding that the two non-
49
50 437 specific acid phosphatases have similar abundance in a UK grassland soil (Neal et al., 2017), Nsap-A was the prevalent
51
52 438 phosphatase in the grasslands included in this study. The predominance of phosphatase on grassland could be affected by
53
54 439 the interaction between microorganism and plant communities since both are able to produce these enzymes (Mhlongo et
55
56 440 al., 2018).

57 441

58
59
60

1
2 442 The relationship study among each P-enzymes abundance and phylogeny with environmental variables demonstrated that
3
4 443 T_{max} , pH and aet were key players in the abundance and phylogenetic distribution of P-enzymes, as it was observed in the
5
6 444 analysis with the general functional profiles (i.e. subsystems level 2). More specifically, the co-variation analyses of P-
7
8 445 enzymes (Table S17) and of P-enzymes with the general functional profiles (Table S18) showed, on the one hand, that the
9
10 446 variation of P-enzymes present a highly interconnected structure between the 8 P-enzymes herein analyzed. On the other
11
12 447 hand, each of the P-enzymes showed a different relationship with the variability of the functional profile in each sample.

13 448
14
15 449 One important question is to understand if the P-enzymes are driven particularly by the change of certain organisms that are
16
17 450 carrying them or, in turn, they are following the general major changes in the community structure. One possible hint in this
18
19 451 direction is given by the comparison of CAP analyses at the subsystem level with the ones of each P-enzyme (Table S18).
20
21 452 Indeed, in this case only PhoD and the two phytases (BPP and Cphy) showed a similar trend in these analyses, indicating
22
23 453 that these enzymes may be accompanying the general change in the functional structure of the metagenome, whilst the other
24
25 454 P-enzymes are varying in a more idiosyncratic manner.

26 455
27
28
29 456 This work studied the abundance and distribution of eight key enzymes involved in P organic cycling. The environmental
30
31 457 variables explained a low proportion of the observed microbial functional diversity. However, T_{max} , pH and aet were related
32
33 458 to the diversity of almost all enzymes. These results are in relation to the geographical global scale of the study. The use of
34
35 459 information from samples from very distant sites determines only the effect on the diversity of the variables with greater
36
37 460 differences among the sites. Likewise, it was possible to identify the effect of other variables with a more localized effect,
38
39 461 such as soil texture and nutrient content, as important determinants of microbial community structure and functions. The
40
41 462 complexity of the studied system requires a combination of approaches and the generation of local data that allow the
42
43 463 understanding of factors affecting the presence of bacteria carrying P-enzymes genes as well as their functionality.

44
45 464
46
47
48 465 Acknowledgments:

49
50 466 We acknowledge Victoria Bonnacarrère for their contribution to the discussion.
51
52 467
53
54
55 468
56
57
58
59
60

1
2 469
3
4 470
5
6 471
7
8 472
9
10 473
11
12 474
13
14 475
15
16
17 476
18
19
20 477
21
22
23 478
24
25
26 479
27
28 480
29
30
31 481
32
33 482
34
35 483
36
37
38 484
39
40 485
41
42 486
43
44
45 487
46
47 488
48
49
50 489
51
52 490
53
54 491
55
56
57
58
59
60

References:

- Achat, D.L., Pousse, N., Nicolas, M., Brédoire, F., Augusto, L. (2016). Soil properties controlling inorganic phosphorus availability: general results from a national forest network and a global compilation of the literature. *Biogeochemistry* 127, 255–272. doi: <https://doi.org/10.1007/s10533-015-0178-0>.
- Alori E.T., Glick, B.R., Babalola, O. (2017). Microbial Phosphorus Solubilization and Its Potential for Use in Sustainable Agriculture..*Front. Microbiol.* 8:971. doi: 10.3389/fmicb.2017.00971
- Amundson, R. (2013). Soil formation. In: Holland HD, Turekian KK (eds) *Treatise on geochemistry*, 2nd edn. Elsevier Science, USA, pp 1–26. doi: <https://doi.org/10.1016/B978-0-08-095975-7.00501-5>.
- Anderson, M. J., Willis, T. J. (2003). Canonical analysis of principal coordinates: A useful method of constrained ordination for ecology. *Ecology*, 84(2), 511–525. doi: [https://doi.org/10.1890/0012-9658\(2003\)084\[0511:CAOPCA\]2.0.CO;2](https://doi.org/10.1890/0012-9658(2003)084[0511:CAOPCA]2.0.CO;2)
- Ariza,A., Moroz, O.V., Blagova, E.V., Turkenburg, J.P., Waterman,J., et al. (2013) Degradation of Phytate by the 6-Phytase from *Hafnia alvei*: A Combined Structural and Solution Study. *PLoS ONE* 8(5): e65062. doi: <https://doi.org/10.1371/journal.pone.0065062>.
- Awasthi,R.,Tewari,R., Nayyar, H. (2011). Synergy between plants and P solubilizing microbes in soils: Effects on growth and physiology of crops. *International Research Journal of Microbiology* 2: 484-503.
- Azeem, M., Riaz, A., Nawaz , A., Hayat, R., Hussain, Q., Tahir, n., Imran, M. (2015) Microbial phytase activity and their role in organic P mineralization, *Archives of Agronomy and Soil Science*, 61:6, 751-766. doi: [10.1080/03650340.2014.963796](https://doi.org/10.1080/03650340.2014.963796)

- 1
2 492 Bachar, A., Al-Ashhab, A., Soares, M.I.M., Sklars, M., Angel, R., Ungar, R., Gillor, O. (2010). Soil microbial abundance
3
4 493 and diversity along a low precipitation gradient. *Microb Ecol* 60:453–461. doi: <https://doi.org/10.1007/s00248-010-9727-1>
5
6
7 494 Barbera, P., Kozlov, A. M., Czech, L., Morel, B., Darriba, D., Flouri, T., Stamatakis, A. (2019). EPA-ng: Massively Parallel
8
9 495 Evolutionary Placement of Genetic Sequences. *Systematic Biology*, 68, 365–369. doi:
10
11 496 <https://doi.org/10.1093/sysbio/syy054>
12
13 497 Barnett K.L., Facey S.L. (2016). Grasslands, Invertebrates, and Precipitation: A Review of the Effects of Climate Change.
14
15 498 *Front. Plant Sci.* 7:1196. doi: 10.3389/fpls.2016.01196
16
17
18 499 Bergkemper, F., Kublik, S., Lang, F., Krüger, J., Vestergaard, G., Schloter, M., Schulz, S. (2016). Novel oligonucleotide
19
20 500 primers reveal a high diversity of microbes which drive phosphorous turnover in soil. *J. Microbiol. Methods* 125, 91–97.
21
22 501 doi:<https://doi.org/10.1016/j.mimet.2016.04.011>.
23
24
25 502 Blair, J., Nippert, J., Briggs, J. (2014). In R.K. Monson (ed.). *Grassland Ecology, Ecology and the Environment*, 389-423.
26
27 503 10.1007/978-1-4614-7501-9_14.
28
29
30 504 Braithwaite, D.T., Keegan, K.P. (2018). matR: Metagenomics Analysis Tools. R package version 0.9.1. [https://CRAN.R-](https://CRAN.R-project.org/package=matR)
31
32 505 [project.org/package=matR](https://CRAN.R-project.org/package=matR).
33
34
35 506 Caffaro, M., Balestrasse, K., Rubio, G. (2020). Adsorption to soils and biochemical characterization of commercial
36
37 507 phytases. *SOIL*. 6. 153-162. doi:10.5194/soil-6-153-2020.
38
39
40 508 Cai, S., Deng, K., Tang, J., Sun, R., Lu, H., Li, et al. (2021). Characterization of extracellular phosphatase activities in
41
42 509 periphytic biofilm from paddy field. *Pedosphere* 31, 116–124. doi:[https://doi.org/10.1016/S1002-0160\(20\)60061-3](https://doi.org/10.1016/S1002-0160(20)60061-3).
43
44
45 510 Condron, L.M., Turner, B.L., Cade-Menun, B.J. (2005). Chemistry and dynamics of soil organic phosphorus. *Phosphorus*
46
47 511 *Agric. Environ.* 46, 87–121. doi: <https://doi.org/10.2134/agronmonogr46.c4>.
48
49
50 512 Cui, H., Sun, W., Delgado-Baquerizo, M., Ma, J.Y., Wang, K., Ling, X. (2022). Phosphorus addition regulates the
51
52 513 responses of soil multifunctionality to nitrogen over-fertilization in a temperate grassland. *Plant Soil* **473**, 73–87. doi:
53 514 <https://doi.org/10.1007/s11104-020-04620-2>.
54
55
56
57
58
59
60

- 1
2 515 Czech, L., Barbera, P., Stamatakis, A. (2020). Genesis and Gappa: processing, analyzing and visualizing phylogenetic
3
4 516 (placement) data. *Bioinformatics*, 36, 3263–3265. doi:<https://doi.org/10.1093/bioinformatics/btaa070>.
5
6
7 517 Dahal, R.H., Kim, J. (2017). *Rhodanobacter humi* sp. nov., an acid-tolerant and alkalitolerant gammaproteobacterium
8
9 518 isolated from forest soil. *Int J Syst Evol Microbiol*, 67, 1185-1190. doi: 10.1099/ijsem.0.001786.
10
11
12 519 Dubeux, J., Sollenberger, L. E., Mathews, B. W. , Scholberg, J. M., Santos, H. Q. (2007). Nutrient Cycling in Warm-
13
14 520 Climate Grasslands. *Crop Sci.* 47:915–928. doi: 10.2135/cropsci2006.09.0581
15
16
17 521 Elser, J., Andersen, T., Baron, J.S., Bergström, AK., Jansson, M., Kyle, M., et al. (2009). Shifts in Lake N:P Stoichiometry
18
19 522 and Nutrient Limitation Driven by Atmospheric Nitrogen Deposition. *Science* , 326, N.º 5954, 835-837. doi:[DOI:
20 523 10.1126/science.1176199](https://doi.org/10.1126/science.1176199).
21
22
23 524
24
25
26 525 Evans, S.N., Matsen, F.A. (2012). The phylogenetic Kantorovich–Rubinstein metric for environmental sequence samples. *J*
27
28 526 *R Stat Soc Series B Stat Methodol*, 74:569–92. doi: [10.1111/j.1467-9868.2011.01018.x](https://doi.org/10.1111/j.1467-9868.2011.01018.x)
29
30
31 527 Fierer, N., Jackson, R.B. (2006). The diversity and biogeography of soil bacterial communities. *Proc Natl Acad Sci*
32
33 528 103:626–631. doi: <https://doi.org/10.1073/pnas.0507535103>
34
35
36 529 Gaiero, J.R., Bent, E., Fraser, T.D., Condrón, L.M., Dunfield, K.E. (2018). Validating novel oligonucleotide primers
37
38 530 targeting three classes of bacterial non-specific acid phosphatase genes in grassland soils. *Plant Soil* 427, 39–51. doi:
39
40 531 <https://doi.org/10.1007/s11104-017-3338-2>.
41
42
43 532 Gaiero, J., Bent, E., Boitt, G., Condrón, L., Dunfield, K. (2020). Effect of long-term plant biomass management on
44
45 533 phosphatase-producing bacterial populations in soils under temperate grassland. *Applied Soil Ecology*, 151, 103583. doi:
46
47 534 <https://doi.org/10.1016/j.apsoil.2020.103583>.
48
49
50 535 Garaycochea, S., Romero, H., Beyhaut, E., Neal, A.L, Altier, N. (2020). Soil structure, nutrient status and water holding
51
52 536 capacity shape Uruguayan grassland prokaryotic communities. *FEMS Microbiology Ecology*, 96, 12. doi:
53 537 <https://doi.org/10.1093/femsec/fiaa207>
54
55
56
57
58
59
60

- 1
2 538 George, T.S., Giles, C., Menezes-Blackburn, D., Condrón, L., Gama-Rodrigues, A.C., Jaisi, D., et al. (2018). Organic
3
4 539 phosphorus in the terrestrial environment: a perspective on the state of the art and future priorities. *Plant Soil* 427, 191–208.
5
6 540 doi: <https://doi.org/10.1007/s11104-017-3391-x>.
7
8
9 541 Gerke, J., (2015). The acquisition of phosphate by higher plants: Effect of carboxylate release by the roots. A critical review.
10
11 542 *J. Plant Nutr. Soil Sci.* 178, 351–364. doi: <https://doi.org/10.1002/jpln.201400590>.
12
13 543 Gu, C., Wilson, S. G., Margenot, A. (2020). Lithological and bioclimatic impacts on soil phosphatase activities in California
14
15 544 temperate forests. *Soil Biology and Biochemistry.* 141, 107633. doi:<https://doi.org/10.1016/j.soilbio.2019.107633>.
16
17
18 545 Gyaneshwar P, Kumar GN, Parekh LJ, Poole PS. (2002). Role of soil microorganisms in improving P nutrition of plants.
19
20 546 *Plant and Soil.* 245:83–93. doi: <https://doi.org/10.1023/A:1020663916259>
21
22
23 547
24
25
26 548 Haygarth, P.M., Bardgett, R.D., Condrón, L.M. (2013). Nitrogen and phosphorus cycles and their management. In: *Soil*
27
28 549 *Conditions and Plant Growth.* Blackwell Publishing Ltd, Oxford, pp. 132–159. doi:
29
30 550 <https://doi.org/10.1002/9781118337295.ch5>.
31
32
33 551 Huang, H., Shi, P., Wang, Y., Luo, H., Shao, N., Wang, G., et al. (2009). Diversity of beta-propeller phytase genes in the
34
35 552 intestinal contents of grass carp provides insight into the release of major phosphorus from phytate in nature. *Appl. Environ.*
36
37 553 *Microbiol.* 75, 1508–1516. doi: <https://doi.org/10.1128/AEM.02188-08>.
38
39
40 554 Islam, W., Noman, A., Naveed, H. Huang, Z., Chen., H.. Role of environmental factors in shaping the soil microbiome.
41
42 555 *Environ Sci Pollut Res.* 27, 41225–41247 (2020). doi: <https://doi.org/10.1007/s11356-020-10471-2>.
43
44 556 Kielak, A.M., Barreto, C.C., Kowalchuk, G.A., Van Veen, J.A., Kuramae, E.E. (2016). The Ecology of Acidobacteria:
45
46 557 Moving beyond Genes and Genomes. *Front. Microbiol.* 7:744. doi: 10.3389/fmicb.2016.00744.
47
48
49 558 Johnston, E.R., Hatt, J.K., He, Z., Wu, L., Guo, X., Luo, Y. et al. (2019). Responses of tundra soil microbial communities to
50
51 559 half a decade of experimental warming at two critical depths. *Proc Natl Acad Sci USA* . doi: 116:15096–15105.
52
53 560 <https://doi.org/10.1073/pnas.1901307116>
54
55
56
57
58
59
60

- 1
2 561 Jorquera, M., Martínez, O., Maruyama, F., Marschner, P., de la Luz Mora, M. (2008). Current and future biotechnological
3
4 562 applications of bacterial phytases and phytase producing bacteria. *Microbes Environ.* 23, 182–191. doi:
5
6 563 <https://doi.org/10.1264/jsme2.23.182>.
7
8
9 564 Katoh, K., Misawa, K., Kuma, K., Miyata, T. (2002). MAFFT: a novel method for rapid multiple sequence alignment based
10
11 565 on fast Fourier transform. *Nucleic Acids Res.* 15, 3059–66. doi: 10.1093/nar/gkf436.
12
13
14 566 Knapp, A. K., Harper, C. W., Danner, B. T., Lett, M. S. (2002). Rainfall variability, carbon cycling, and plant species
15
16 567 diversity in a mesic grassland. *Science* 298, 2202–2205. doi: 10.1126/science.1076347.
17
18
19 568 Kozlov, A.M., Darriba, D., Flouri, T., Morel, B., Stamatakis, A. (2019). RAxML-NG: a fast, scalable and user-friendly tool
20
21 569 for maximum likelihood phylogenetic inference. *Bioinformatics*, 35, 4453–4455. doi:
22
23 570 <https://doi.org/10.1093/bioinformatics/btz305>
24
25 571
26
27
28 572 Lauber, C.L., Ramirez, K.S., Aanderud, Z., Lennon, J., Fierrer, N. (2013) Temporal variability in soil microbial
29
30 573 communities across land-use types. *ISME J* 7:1641–1650. <https://doi.org/10.1038/ismej.2013.50>
31
32
33 574 Le Roux, X., Recous, S., Attard, E. 2011. Soil microbial diversity in grasslands, and its importance for grassland
34
35 575 functioning and services. In G. Lemaire and A. Chabbi. (eds). *Grassland Productivity and Ecosystem Services*. CABI
36
37 576 International, Wallingford, UK, 158–165.
38
39
40 577 Lenhart, P. A., Eubanks, M. D., and Behmer, S. T. (2015). Water stress in grasslands: dynamic responses of plants and
41
42 578 insect herbivores. *Oikos* 124, 381–390. doi:10.1111/oik.01370.
43
44
45 579 Letunic, I., Bork, P. (2007). Interactive Tree of Life (iTOL): an online tool for phylogenetic tree display and annotation.
46
47 580 *Bioinformatics*, 23, 127–8. doi: 10.1093/bioinformatics/btl529
48
49
50 581 Li, Y. F., Luo, A. C., Wei, X. H., Yao, X. G. (2008). Changes in phosphorus fractions, pH, and phosphatase activity in the
51
52 582 rhizosphere of two rice genotypes, *Pedosphere*, 18, 785–794. doi: [https://doi.org/10.1016/S1002-0160\(08\)60074-0](https://doi.org/10.1016/S1002-0160(08)60074-0).
53
54
55 583 Li, Y., Niu, S., Yu, G. (2015). Aggravated phosphorus limitation on biomass production under increasing nitrogen loading:
56
57 584 a meta-analysis. *Glob Chan Biol*, 22, 934–943. doi: <https://doi.org/10.1111/gcb.13125>.
58
59
60

- 1
2 585 Li, J., Xie, T., Zhu, H., Zhou, J., Li, c., Xiong, W., et al. (2021). Alkaline phosphatase activity mediates soil organic
3
4 586 phosphorus mineralization in a subalpine forest ecosystem, *Geoderma*, 404, 115376. doi:
5
6 587 <https://doi.org/10.1016/j.geoderma.2021.115376>.
7
8
9 588 Lim, B.L., Yeung, P., Cheng, C., Hill, J.E. (2007). Distribution and diversity of phytate-mineralizing bacteria. *ISME J*
10
11 589 1:321–330. doi: <https://doi.org/10.1038/ismej.2007.40>.
12
13
14 590 Love, M.I., Huber, W., Anders, S. Moderated estimation of fold change and dispersion for RNA-seq data with DESeq2.
15
16 591 (2014). *Genome Biol*, 15:550. doi: <https://doi.org/10.1186/s13059-014-0550-8>.
17
18 592
19
20
21 593 Margalef, O., Sardans, J., Fernández-Martínez, M., Molowny-Horas, R., Janssens, I. A., Ciais, P., et al. (2017). Global
22
23 594 patterns of phosphatase activity in natural soils. *Sci Rep* 7, 1337. doi: <https://doi.org/10.1038/s41598-017-01418-8>.
24
25
26 595 Matsen, F.A., Evans, S.N. (2013). Edge principal components and squash clustering: using the special structure of
27
28 596 phylogenetic placement data for sample comparison. *PLoS One*, 8:e56859.
29
30 597 doi:<https://doi.org/10.1371/journal.pone.0056859>
31
32
33 598 McInnes, L., Healy, J., Melville, J. (2018). UMAP: Uniform Manifold Approximation and Projection for Dimension
34
35 599 Reduction. *Stat and ML*, arXiv:1802.03426v3. doi: <https://doi.org/10.48550/arXiv.1802.03426>.
36
37
38 600 Mhlongo, M.I., Piater, L.A., Madala, N.E., Labuschagne, N., Dubery, I.A. (2018). The Chemistry of Plant–Microbe
39
40 601 Interactions in the Rhizosphere and the Potential for Metabolomics to Reveal Signaling Related to Defense Priming and
41
42 602 Induced Systemic Resistance. *Front. Plant Sci.* 9:112. doi: 10.3389/fpls.2018.00112
43
44
45 603 Minh, B., Schmidt, H., Chernomor, O., Schrempf, D., Woodhams, M., Von Haeseler, A., Lanfear, R. (2020). IQ-TREE 2:
46
47 604 New Models and Efficient Methods for Phylogenetic Inference in the Genomic Era. *Molecular Biology and Evolution*, 37,
48
49 605 1530–1534. doi: <https://doi.org/10.1093/molbev/msaa015>.
50
51
52 606 Misset, O.: Phytase, in: *Handbook of Food Enzymology*, edited by: Whitaker, J., Voragen, A., and Wong, D., Boca Raton,
53
54 607 CRC Press, (2002) 687–706. doi:<https://doi.org/10.1201/9780203910450>.
55
56
57
58
59
60

- 1
2 608 Morrison, E., Newman, S., Bae, H.S., He, Z., Zhou, J., Reddy, K.R., Ogram, A. (2016). Microbial genetic and enzymatic
3
4 609 responses to an anthropogenic phosphorus gradient within a subtropical peatland. *Geoderma* 268, 119–127. doi:
5
6 610 <https://doi.org/10.1016/j.geoderma.2016.01.008>.
7
8
9 611 Morya, R., Salvachúa, D., Thakur, I. S. (2020). Burkholderia: An Untapped but Promising Bacterial Genus for the
10
11 612 Conversion of Aromatic Compounds. *Trends in Biotechnol.* 38, 9: 963-975. doi:
12
13 613 <https://doi.org/10.1016/j.tibtech.2020.02.008>
14
15 614 Nannipieri, P., Giagnoni, L., Landi, L., Renella, G. (2011). Role of phosphatase enzymes in soil. In: *Phosphorus in Action.*
16
17 615 *Soil Biology* Springer, Heidelberg, 215–243. doi:10.1007/978-3-642-15271-9_9
18
19
20 616
21
22
23 617 Neal, A.L., Rossmann, M., Brearley, C., Akkari, E., Guyomar, C., Clark, I., et al. (2017). Land-use influences phosphatase
24
25 618 gene microdiversity in soils. *Environ Microbiol.* 19:2740–753. doi:10.1111/1462-2920.13778
26
27
28 619 Neal, A. L., Blackwell, M. S. A., Akkari, E., Clark, I. M., Hirsch, P. R. and Guyomar, C. (2018). Phylogenetic distribution,
29
30 620 biogeography and the effects of land management upon bacterial non-specific Acid phosphatase Gene diversity and
31
32 621 abundance. *Plant and Soil.* 427, 175-189. doi:<https://doi.org/10.1007/s11104-017-3301-2> .
33
34
35 622 Neal, A. L., McLaren, T., Lourenço Campolino, M., David, H., Marcos Coelho, A., Gomes de Paula Lana, U., et al. (2021).
36
37 623 Crop type exerts greater influence upon rhizosphere phosphohydrolase gene abundance and phylogenetic diversity than
38
39 624 phosphorus fertilization. *FEMS Microbiol. Ecol.*, 97, 4. doi: <https://doi.org/10.1093/femsec/fiab033>
40
41
42 625 Ochoa,M.S., Pedraza, R.M., Martínez, M. (2010). Plantas, hongos micorrízicos y bacterias : su compleja red de
43
44 626 interacciones. *Biológicas* 12:65–71.
45
46
47 627 Oksanen, J., Blanchet, F.G., Kindt, R., Legendre, P., Minchin, P.R., O'Hara, R.B. et al. Vegan: community ecology
48
49 628 package. R package version 2.62. <https://CRAN.R-project.org/package=vegan>, 08/15/2022.
50
51
52 629 Peñuelas, J., Poulter, B., Sardans, J., Philippe, C., Van der Velde, M., Laurent, B. et al. (2013) Human-induced nitrogen–
53
54 630 phosphorus imbalances alter natural and managed ecosystems across the globe. *Nat Commun* 4, 2934. doi:
55 631 <https://doi.org/10.1038/ncomms3934>.
56
57
58
59
60

- 1
2 632 Quiquampoix H, Mousain D. (2005). Enzymatic hydrolysis of organic phosphorus. In: Turner BL, Frossard E, Baldwin D,
3
4 633 (eds). Organic phosphorus in the environment. Wallingford (UK): CABI, 89–112. doi:
5
6 634 <https://doi.org/10.1079/9780851998220.0089>.
7
8
9 635 Ragot, S., Kertesz, M., Bünemann, E. (2015). *phoD* Alkaline Phosphatase Gene Diversity in Soil. Applied and
10
11 636 Environmental Microbiology. doi: 10.1128/AEM.01823-15.
12
13 637 Ragot, S., Kertesz, M., Mészáros, E., Frossard, E., Bünemann, E. (2017). Soil *phoD* and *phoX* alkaline phosphatase gene
14
15 638 diversity responds to multiple environmental factors, FEMS Microbiology Ecology. 93, 1. doi:
16
17 639 <https://doi.org/10.1093/femsec/fw212>
18
19
20 640 Rao, M.A., Violante, A., Gianfreda, L. (1994). Catalytic behavior of acid phosphatase immobilized on clay minerals and
21
22 641 organo-mineral complexes transactions. In: 15th World Congress of Soil Science; volumen 3b. International Soil Science
23
24 642 Society, Mexico. Acapulco (Mexico): Mexican Society of Soil Science; 117–118.
25
26
27 643 Richardson, A., Simpson, R. (2011). Soil microorganisms mediating phosphorus availability. Plant Physiol. 156: 989-996.
28
29 644 doi: [10.1104/pp.111.175448](https://doi.org/10.1104/pp.111.175448).
30
31
32 645 Rodriguez, H., Fraga, R., Gonzalez, T., Bashan, Y. (2006). Genetics of phosphate solubilization and its potential
33
34 646 applications for improving plant growth-promoting bacteria. Plant Soil 287, 15–21. doi: 10.1007/978-1-4020-5765-6_2
35
36
37 647 Rodriguez, F., Lillington, J., Johnson, S., Timmel, C. R., Lea, S. M., Berks, B. C. (2014). Crystal structure of the *Bacillus*
38
39 648 *subtilis* phosphodiesterase PhoD reveals an iron and calcium-containing active site. J Biol Chem, 289, 30889–30899. doi:
40
41 649 [10.1074/jbc.M114.604892](https://doi.org/10.1074/jbc.M114.604892)
42
43
44 650 Rossolini, G.M., Schippa, S., Riccio, M.L., Berlutti, F., Macaskie, L.E., Thaller, M.C. (1998). Bacterial nonspecific acid
45
46 651 phosphohydrolases: physiology, evolution and use as tools in microbial biotechnology. Cell Mol Life Sci. 54: 833-850. doi:
47
48 652 [10.1007/s000180050212](https://doi.org/10.1007/s000180050212)
49
50
51 653 Santos-Beneit, F. (2015). The Pho regulon: A huge regulatory network in bacteria. Front. Microbiol, 6, 402. doi:
52
53 654 [10.3389/fmicb.2015.00402](https://doi.org/10.3389/fmicb.2015.00402).
54
55
56 655 Saxena, A.K., Kumar, M., Chakdar, H., Anuroopa, N., Bagyaraj, D.J. (2020). *Bacillus* species in soil as a natural resource
57
58 656 for plant health and nutrition. J Appl Microbiol. 128(6):1583-1594. doi: 10.1111/jam.14506.
59
60

- 1
2 657 Sebastian, M., Ammerman, J.W. (2011). Role of the phosphatase PhoX in the phosphorus metabolism of the marine
3
4 658 bacterium *Ruegeria pomeroyi* DSS-3. *Environ Microbiol Rep* 3:535–542. doi: 10.1111/j.1758-2229.2011.00253.x.
5
6
7 659 Seshachala, U., Tallapragada, P. (2012). Phosphate solubilizers from the rhizosphere of *Piper nigrum* L. in Karnataka, India.
8
9 660 *Chil. J. Agric. Res.* 72, 397–403. doi: 10.4067/S0718-58392012000300014.
10
11 661
12
13
14 662 Sorensen, P.O., Bhatnagar, J.M., Christenson, L. Duran, J., Fahey, T., Fisk, M. et al. (2019). Roots mediate the effects of
15
16 663 snowpack decline on soil bacteria, fungi, and nitrogen cycling in a northern hardwood forest. *Front Microbiol* 10:926. doi:
17
18 664 <https://doi.org/10.3389/fmicb.2019.00926>.
19
20
21 665 Spohn, M., Kuzyakov, Y. (2013). Phosphorus mineralization can be driven by microbial need for carbon. *Soil Biology and*
22
23 666 *Biochemistry*, 61, 69–75. doi: <https://doi.org/10.1016/J.SOILBIO.2013.02.013>
24
25
26 667 Tan, H., Barret, M., Mooij, M.J., Rice, O., Morrissey, J., Dobson, A., et al. (2013). Long-term phosphorus fertilisation
27
28 668 increased the diversity of the total bacterial community and the *phoD* phosphorus mineraliser group in pasture soils. *Biol*
29
30 669 *Fertil Soils* 49, 661–672. doi: <https://doi.org/10.1007/s00374-012-0755-5>.
31
32
33 670 Tang, J., Leung, A., Leung, C., Lim, B.L. (2006). Hydrolysis of precipitated phytate by three distinct families of phytases.
34
35 671 *Soil Biol Chem.* 38:1316–1324. doi: <https://doi.org/10.1016/j.soilbio.2005.08.021>.
36
37
38 672 Tecon, R., Or, D. (2017). Biophysical processes supporting the diversity of microbial life in soil. *FEMS Microbiol Rev*
39
40 673 41:599–623. doi:<https://doi.org/10.1093/femsre/fux039>
41
42
43 674 Thaller, M.C., Schippa, S., Rossolini, G.M. (1998). Conserved sequence motifs among bacterial, eukaryotic and archaeal
44
45 675 phosphatases that define a new phosphohydrolase superfamily. *Protein Sci.* 1998; 7: 1647-1652. doi:
46 676 [10.1002/pro.5560070722](https://doi.org/10.1002/pro.5560070722).
47
48
49 677 Tu, S.M.L., Ma, L., Rathinasabapathi, B. (2011). Characterization of phytase from three ferns with differing arsenic
50
51 678 tolerance. *Plant Physiol Biochem.* 49:146–150. doi: <https://doi.org/10.1016/j.plaphy.2010.11.004>.
52
53
54
55
56
57
58
59
60

- 1
2 679 Wei, X., Hu, Y., Cai, G., Yao, H., Ye, J., Sun, Q., et al. (2021). Organic phosphorus availability shapes the diversity of
3
4 680 phoD-harboring bacteria in agricultural soil. *Soil Biol Biochem.* 161, 108364. doi:
5
6 681 <https://doi.org/10.1016/j.soilbio.2021.108364>.
7
8
9 682 Weon, H., Anandham, R., Kim, B., Hong, S., Jeon, Y., Kwon, S. (2009). *Dyella soli* sp. nov. and *Dyella terrae* sp. nov.,
10
11 683 isolated from soil. *Int. J. Syst. Evol. Microbiol.* 59, 1685–1690. doi: <https://doi.org/10.1099/ijs.0.004838-0>.
12
13 684
14
15
16 685 White, R.P., Murray, S., Rohweder, M., Prince, S., Thompson, K. (2000). *Grassland ecosystems*. World Resources Institute.
17
18 686 Washington DC, U.S.A.
19
20
21 687 Wickham H. *ggplot2: Elegant Graphics for Data Analysis*. Springer Verlag: New York. 2016.
22
23
24 688 Wilke, A., Bischof, J., Harrison, T., Brettin, T., D'Souza, M., Gerlach W, et al. (2015) A RESTful API for Accessing
25
26 689 Microbial Community Data for MG-RAST. *PLoS Comput Biol* 11(1): e1004008.
27
28 690 <https://doi.org/10.1371/journal.pcbi.1004008>
29
30
31 691 Yao, M.Z., Zhang, Y.H., Lu, W.L., Hu, M.Q., Wang, W., Liang, A.H. (2012). Phytases: crystal structures, protein
32
33 692 engineering and potential biotechnological applications. *J Appl Microbiol* 112:1–14. doi:10.1111/j.1365-2672.2011.05181.x
34
35
36 693 Zhou, Q., Daryanto, S., Xin, Z., Liu, Z., Liu, M., Cui, X., Wang, L. (2017). Soil phosphorus budget in global grasslands and
37
38 694 implications for management. *Journal of Arid Environments*. 144. 10.1016/j.jaridenv.2017.04.008.
39
40 695
41
42 696
43
44 697
45
46 698
47
48 699
49 700
50
51 701
52
53 702
54
55 703
56
57 704
58
59
60

1
2 705 Tables legends:

3
4 706

5
6 707 **Table 1:** List of P-enzymes included in the analyses.

7
8 708 **Table 2:** Canonical Correlation Analysis (CAP) summaries. CAP analyses based on Mahalanobis distance for MG-RAST
9
10 709 level 2 subsystem annotations and enzyme abundance and based on Kantorovich-Rubinstein distance for each of eight
11 710 enzymes. Environmental variables included: pH, Soil Organic Carbon (SOC), Phosphorous estimated (Pav), Cation
12
13 711 Exchange Capacity (CEC), Bulk Density (BD), Clay, Sand, silt, actual evapotranspiration (aet), runoff (q), soil moisture
14
15 712 (moisture), precipitation (ppt), maximum Temperature (T_{max}). PERMANOVA analysis with 999 permutations was
16
17 713 performed to determine the significance between the sites/MG-RAST project. The values marked with red are significant.
18

19 714

20
21 715 Figures legends:

22
23 716

24
25 717 **Figure 1:** Phylogenetic placements of the predicted proteins of each metagenome with respect to the reference bases of
26
27 718 each enzyme: a) PhoD, b) PhoX, c) Nsap-A and d) BPP The size of the circle representing placements is proportional to the
28
29 719 abundance. Maximum likelihood-based phylogenetic placement of metagenome-derived protein sequences was performed
30
31 720 with EPA-ng and tree drawn with iTOL. The circle sizes represent the number of hits per node.
32

33 721

34
35 722

36
37 723

38
39 724 **Figure 2:** CAP based on Kantorovich-Rubinstein distance for PhoD. PERMANOVA analysis with 999 permutations was
40
41 725 performed to determine the significance between the sites/MG-RAST project. For each MG-RAST project three samples
42
43 726 with the same geo-reference were included. Each point represents samples from the project mpg1992 (blue); mpg3520
44
45 727 (green); mpg5588 (dark red); mpg7792 (grey); mpg8624 (mustard); mgp9904 (violet); mgp10450 (dark blue); mgp10523
46
47 728 (stone blue); mgp10541 (turquoise); mgp10956 (yellow); mgp13011 (lilac); mgp13520 (jade); mpg13948(orange);
48
49 729 mpg20922 (brown); mgp89409 (brick-red); mgp91922. (light green); mgp93346 (light blue). Vector lengths represent the
50
51 730 correlation between each variable and the axes. CAP analysis was performed with the Vegan R package and graphics were
52
53 731 produced with the R package ggplot2.
54

55
56 732

57
58 733

59
60

1
2 734
3
4 735 **Figure 3:** Correlation matrix of KR-CAP axes. a) Correlogram of the alkaline phosphatases displays the pearson correlation
5
6 736 coefficients between KR-CAP PhoD axes, KR-CAP PhoX and KR-CAP PhoA; KR-CAP PhoX and KR-CAP PhoA. The
7
8 737 correlation coefficients are colored according to their values; being blue the positives values and red the negative values. b)
9
10 738 Correlogram of the acid phosphatases displays the Pearson correlation coefficients between KR-CAP Nsap-A axes, KR-
11
12 739 CAP Nsap-B and KR-CAP Nsap-C; KR-CAP Nsap-B and KR-CAP Nsap-C. The correlation coefficients are colored
13
14 740 according to their values; being blue the positives values and red the negative values. c) Correlogram of the phytases
15
16 741 displays the Pearson correlation coefficients between KR-CAP BPP axes and KR-CAP CPhy. The correlation coefficients
17
18 742 are colored according to their values; being blue the positives values and red the negative values. d) Correlogram of the
19
20 743 most abundance displays the Pearson correlation coefficients. The correlation coefficients are colored according to their
21
22 744 values; being blue the positives values and red the negative values. Correlation analysis and graphics were performed with
23
24 745 cor R package.

25 746
26
27 747
28
29 748
30
31 749 **Figure 4:** a) Graphic representation of the first two axes of the edge-PCA for PhoD using samples as observations. Each
32
33 750 point represents samples from the project mpg1992 (blue); mpg3520 (green); mpg5588 (dark red); mpg7792 (gray);
34
35 751 mpg8624 (mustard); mgp9904 (violet); mgp10450 (dark blue); mgp10523 (stone blue); mgp10541 (turquoise); mgp10956
36
37 752 (yellow); mgp13011 (lilac); mgp13520 (jade); mpg13948(orange); mpg20922 (brown); mgp89409 (brick-red); mgp91922
38
39 753 (light green); mgp93346 (light blue). b) The phylogeny distribution of PhoD hits along the first and second axis of the
40
41 754 analysis (protein with positive coefficients are marked in blue and proteins with negative coefficients are marked in orange).
42
43 755 The edge-PCA was performed using gappa software and tree and domain composition diagrams were drawn using
44
45 756 Archaeopteryx (<https://sites.google.com/site/cmzmasek/home/software/forester>).

46 757
47
48 758
49
50 759
51
52 760
53
54 761
55

56
57
58
59
60

Hoja 1

Table 1: Canonical Correlation Analysis (CAP) summary.

Canonical Correlation Analysis (CAP) summaries. CAP analyses based on Mahalanobis distance for MG-R/ or each of eight enzymes. Environmental variables included: pH, Soil Organic Carbon (SOC), Phosphorous runoff (q), soil moisture (moisture), precipitation (ppt), maximum Temperature (T_{max}). PERMANOVA analysis. The values marked with red are significant.

Summary CAP analysis Subsystems vs. environmental variables

Variables	p-value	CAP1 (r)	CAP2 (r)
pH	0.001	-0.743388	-0.48557
SOC	0.001	0.5641573	-0.22026
Pav	0.059	0.5685315	-0.29112
CEC	0.057	0.15248293	-0.15898
BD	0.001	-0.520975	-0.11709
Clay	0.001	-0.04241	0.230605
Sand	0.001	0.1199085	0.072694
Silt	0.07	-0.1405	-0.30992
aet	0.001	0.6470976	0.182659
q	0.001	0.569242	0.489641
moisture	0.002	0.535826	0.476092
ppt	0.128	0.6497948	0.359254
Tmax	0.01	-0.160555	0.663534

Significant level: < 0.05

Summary Enzymes abundance vs. environmental variables

Variables	p-value	CAP1 (r)	CAP2 (r)
pH	0.001	-0.6973	-0.27085
SOC	0.009	0.5183	0.20957
Pav	0.004	0.5169	0.11622
CEC	0.086	0.2813	0.03614
BD	0.001	-0.4785	-0.33867
Clay	0.003	0.1162	0.18492
Sand	0.001	-0.3984	-0.0248
Silt	0.001	0.4854	-0.12494
aet	0.03	0.6699	0.37789
q	0.002	0.7218	0.39268
moisture	0.079	0.8154	0.11556
ppt	0.014	0.7442	0.41054
Tmax	0.001	0.1773	-0.40276

Significant level: < 0.05

Summary KR-CAP

Variables	p-value	Nsap - A		Nsap - B	
		CAP1 (r)	CAP2 (r)	p-value	CAP1 (r)
pH	0.03	0.05717	0.2724	0.12	0.47
SOC	0.05	-0.1112	-0.1827	0.52	-0.64
Pav	0.20	-0.1772	-0.1745	0.19	-0.60
CEC	0.00	-0.3802	0.2268	0.91	-0.43
BD	0.03	0.0921	0.1284	0.00	0.65
Clay	0.06	0.08635	-0.3534	0.65	-0.30

1
2
3
4
5
6
7
8
9
10
11
12
13
14
15
16
17
18
19
20
21
22
23
24
25
26
27
28
29
30
31
32
33
34
35
36
37
38
39
40
41
42
43
44
45
46
47
48
49
50
51
52
53
54
55
56
57
58
59
60

Hoja1

Sand	0.00	0,1726	0,3906	0.03	0.40
Silt	0.00	-0,3365	-0,2576	0.47	-0.34
aet	0.00	0,01457	-0,4331	0.85	-0.59
q	0.05	-0,01404	-0,4632	0.00	-0.80
mositure	0.07	-0,2714	-0,5149	0.16	-0.68
ppt	0.08	0,0009	-0,4779	0.41	-0.75
Tmax	0.00	-0,2399	-0,1687	0.51	0.09

	p-value	% variance	p-value	% variance
CAP model	0.001	33.7	0.05	32.6
CAP 1 axis	0.001	11.54	0.001	11.6
CAP2 axis	0.01	4.2	0.889	4.1

Significant level: < 0.05

Variables	PhoA			PhoD	
	p-value	CAP1 (r)	CAP2 (r)	p-value	CAP1 (r)
pH	0.07	-0.03522	-0.29193	0.001	-0.7458
SOC	0.10	-0.18357	0.11853	0.001	0.2215
Pav	0.33	0.11462	-0.35058	0.057	0.1815
CEC	0.02	0.04626	0.45434	0.001	-0.2168
BD	0.43	0.43246	-0.05363	0.001	-0.3912
Clay	0.07	-0.16675	-0.03886	0.002	0.1614
Sand	0.57	-0.34526	0.38053	0.001	-0.2812
Silt	0.46	-0.02365	0.38981	0.001	0.2735
aet	0.02	0.11362	0.45529	0.001	0.7788
q	0.58	0.15956	0.39767	0.05	0.7199
mositure	0.58	-0.10224	0.10328	0.033	0.7656
ppt	0.46	0.14536	0.45321	0.092	0.8016
Tmax	0.06	-0.17885	-0.51421	0.001	0.313

	p-value	% variance	p-value	% variance
CAP model	0.001	13	0.001	49.8
CAP 1 axis	0.026	8.7	0.001	19.8
CAP2 axis	0.568	3.9	0.001	12.9

Variables	BPP				
	CAP2 (r)	p-value	CAP1 (r)	CAP2 (r)	p-value
pH	-0.08319	0.001	0.43753	0.05546	0.01
SOC	-0.36845	0.066	-0.28013	-0.4779	0.193
Pav	-0.30488	0.048	-0.33169	-0.52562	0.007
CEC	-0.25386	0.001	-0.36934	-0.61884	0.01
BD	0.17916	0.002	0.26955	0.3567	0.122
Clay	0.02404	0.022	-0.09218	0.04861	0.526
Sand	-0.05236	0.001	0.27865	0.2573	0.222
Silt	0.06312	0.002	-0.35365	-0.46807	0.302
aet	-0.11494	0.004	-0.30758	-0.36789	0.928
q	-0.45532	0.012	-0.36536	0.06208	0.002
mositure	-0.11568	0.169	-0.62166	-0.22685	0.03
ppt	-0.30633	0.164	-0.35532	-0.1892	0.42
Tmax	0.04016	0.001	-0.28546	0.77029	0.508

	p-value	% variance	p-value
--	---------	------------	---------

1				
2		Hoja1		
3				
4	CAP model	0.001	47	0.03
5	CAP 1 axis	0.001	23	0.01
6	CAP2 axis	0.002	5	0.1
7				
8				
9				
10				
11				
12				
13				
14				
15				
16				
17				
18				
19				
20				
21				
22				
23				
24				
25				
26				
27				
28				
29				
30				
31				
32				
33				
34				
35				
36				
37				
38				
39				
40				
41				
42				
43				
44				
45				
46				
47				
48				
49				
50				
51				
52				
53				
54				
55				
56				
57				
58				
59				
60				

For Review Only

Hoja1

AST level 2 Subsystem annotations and Enzyme abundance and based on Kantorovich-Rubinstein dis
 estimated (Pav), Cation Exchange Capacity (CEC), Bulk Density (BD), Clay, Sand, silt, actual evapotra
 ; with 999 permutations was performed to determine the significance between the sites/MG-RAST proje

For Review Only

	CAP2 (r)	p-value	Nsap-C	
	-0.28	0.01	0.140754	0.12030
	-0.19	0.02	0.022451	-0.26188
	-0.27	0.11	-0.021009	-0.27642
	-0.07	0.16	0.015907	-0.00817
	0.16	0.03	0.069241	0.43017
	0.14	0.00	0.184619	-0.68596

Hoja1

1				
2				
3				
4	-0.05	0.03	-0.020522	0.52716
5	-0.06	0.10	-0.160945	-0.12524
6	0.32	0.00	0.169356	-0.20919
7	0.27	0.02	0.003874	-0.36095
8	0.19	0.04	-0.16822	2 -0.45512
9	0.32	0.01	0.09004	9 -0.30461
10	0.31	0.00	-0.49931	1 -0.03969

p-value

11				
12				
13	0.001		35.7	
14	0.001		13.9	
15	0.009		4.7	
16				
17				
18				
19				

PhoX

20				
21	CAP2 (r)	p-value	CAP1 (r)	
22	0.05607	0.008	0.12366	
23	-0.09641	0.007	-0.04539	
24	-0.14912	0.038	-0.07951	
25	-0.17404	0.041	-0.08377	
26	0.16044	0.074	0.02727	
27	-0.01658	0.01	0.27152	
28	0.16174	0.017	-0.0915	
29	-0.22271	0.142	-0.09713	
30	0.01391	0.001	0.27686	
31	-0.071	0.055	0.00448	
32	-0.2901	0.085	-0.17901	
33	-0.0304	0.146	0.15543	
34	-0.4091	0.001	-0.61055	
35				

p-value

% variance

36				
37				
38	0.001		41.4	
39	0.001		19	
40	0.05		4.7	
41				
42				

Cphy

43				
44	CAP1 (r)	CAP2 (r)		
45	0.56979	0.289629		
46	-0.26451	-0.17929		
47	-0.33896	-0.164919		
48	-0.32083	-0.417049		
49	0.36079	0.104345		
50	0.18956	-0.038679		
51	-0.11115	0.128107		
52	0.02804	-0.159731		
53	-0.48723	-0.474511		
54	-0.33336	-0.375057		
55	-0.67975	-0.40317		
56	-0.43992	-0.45665		
57	0.14755	0.00358		
58				

% variance

1
2
3
4
5
6
7
8
9
10
11
12
13
14
15
16
17
18
19
20
21
22
23
24
25
26
27
28
29
30
31
32
33
34
35
36
37
38
39
40
41
42
43
44
45
46
47
48
49
50
51
52
53
54
55
56
57
58
59
60

Hoja1

49.5
10.7
7.6

For Review Only

1
2
3
4
5
6
7
8
9
10
11
12
13
14
15
16
17
18
19
20
21
22
23
24
25
26
27
28
29
30
31
32
33
34
35
36
37
38
39
40
41
42
43
44
45
46
47
48
49
50
51
52
53
54
55
56
57
58
59
60

Hoja1

stance f
anspiration (aet),
ect.

For Review Only

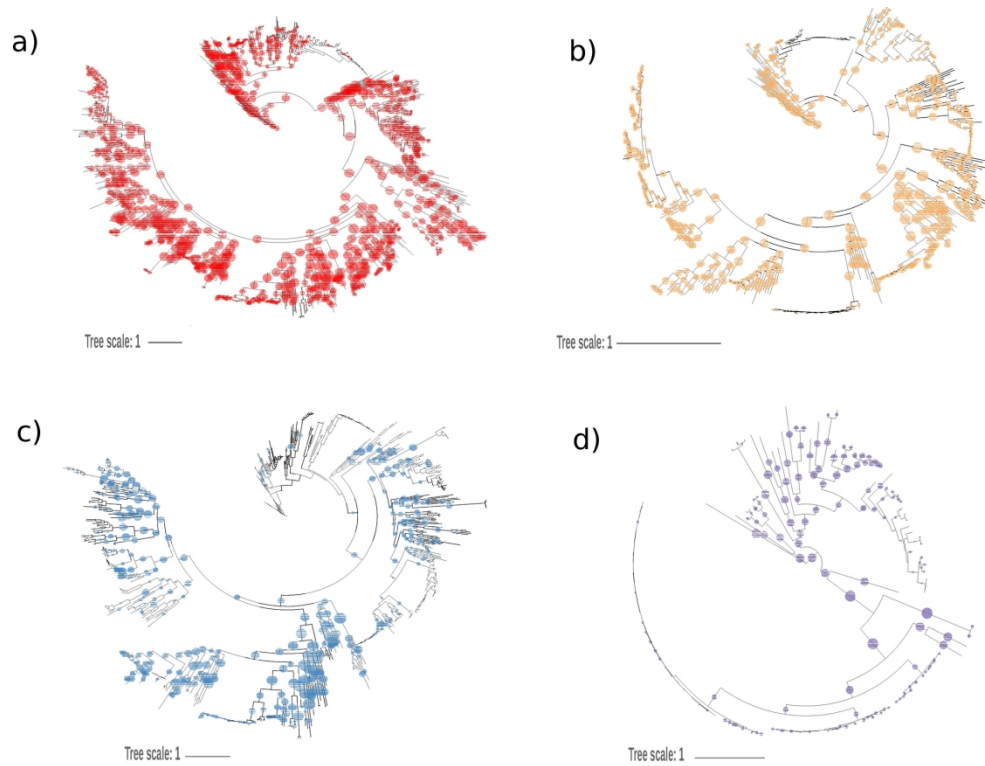


Figure 1: Phylogenetic placements of the predicted proteins of each metagenome with respect to the reference bases of each enzyme: a) PhoD, b) PhoX, c) Nsap-A and d) BPP The size of the circle representing placements is proportional to the abundance. Maximum likelihood-based phylogenetic placement of metagenome-derived protein sequences was performed with EPA-ng and tree drawn with iTOL. The circle sizes represent the number of hits per node.

Phylogenetic placements of the predicted proteins of each metagenome with respect to the reference bases of each enzyme: a) PhoD, b) PhoX, c) Nsap-A and d) BPP The size of the circle representing placements is proportional to the abundance. Maximum likelihood-based phylogenetic placement of metagenome-derived protein sequences was performed with EPA-ng and tree drawn with iTOL. The circle sizes represent the number of hits per node.

183x178mm (300 x 300 DPI)

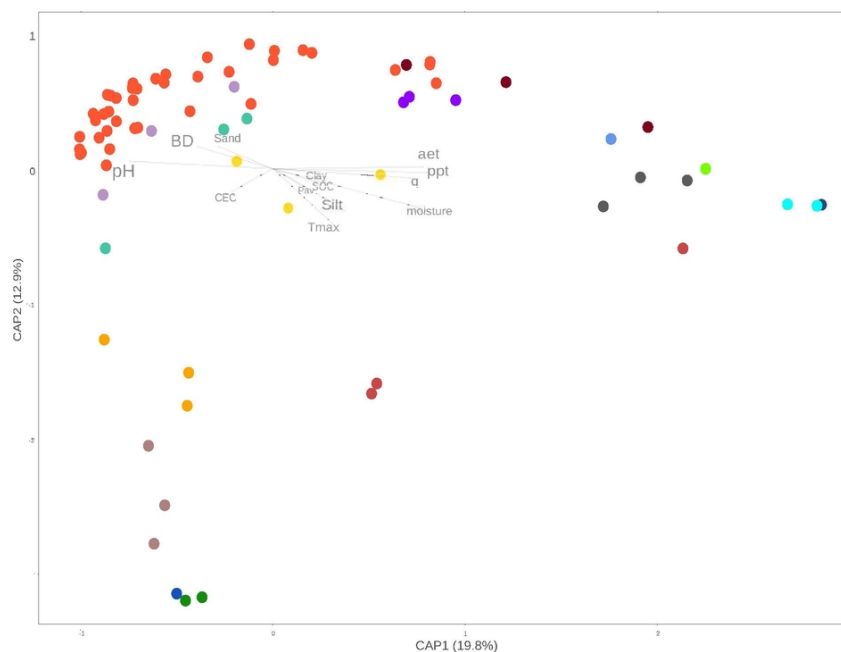


Figure 2: CAP based on Kantorovich-Rubinstein distance for PhoD. PERMANOVA analysis with 999 permutations was performed to determine the significance between the sites/MG-RAST project. For each MG-RAST project three samples with the same geo-reference were included. Each point represents samples from the project mpg1992 (blue); mpg3520 (green); mpg5588 (dark red); mpg7792 (grey); mpg8624 (mustard); mpg9904 (violet); mpg10450 (dark blue); mpg10523 (stone blue); mpg10541 (turquoise); mpg10956 (yellow); mpg13011 (lilac); mpg13520 (jade); mpg13948 (orange); mpg20922 (brown); mpg89409 (brick-red); mpg91922. Vector lengths represent the correlation between each variable and the axes. CAP analysis was performed with the Vegan R package and graphics were produced with the R package ggplot2.

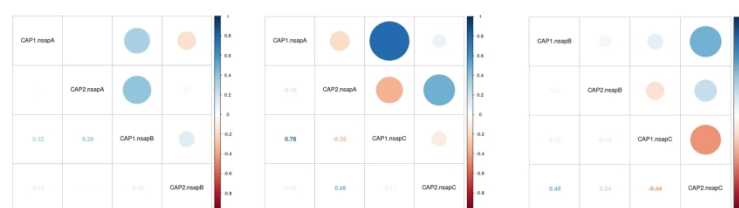
CAP based on Kantorovich-Rubinstein distance for PhoD. PERMANOVA analysis with 999 permutations was performed to determine the significance between the sites/MG-RAST project. For each MG-RAST project three samples with the same geo-reference were included. Each point represents samples from the project mpg1992 (blue); mpg3520 (green); mpg5588 (dark red); mpg7792 (grey); mpg8624 (mustard); mpg9904 (violet); mpg10450 (dark blue); mpg10523 (stone blue); mpg10541 (turquoise); mpg10956 (yellow); mpg13011 (lilac); mpg13520 (jade); mpg13948 (orange); mpg20922 (brown); mpg89409 (brick-red); mpg91922. (light green); mpg93346 (light blue). Vector lengths represent the correlation between each variable and the axes. CAP analysis was performed with the Vegan R package and graphics were produced with the R package ggplot2.

81x113mm (300 x 300 DPI)

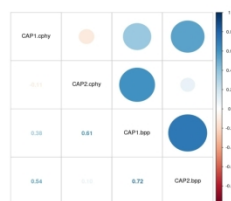
a) alkaline phosphatases



b) Non-specific acid phosphatases



c) Phytases



d) Most abundant

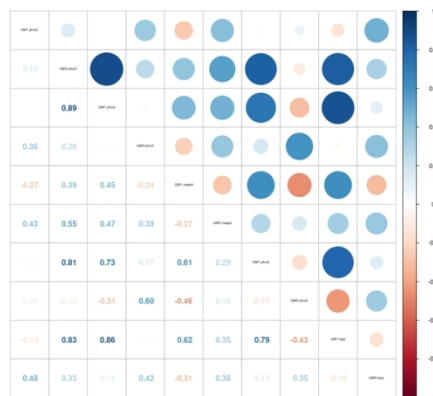


Figure 3: Correlation matrix of KR-CAP axes. a) Correlogram of the alkaline phosphatases displays the Pearson correlation coefficients between KR-CAP PhoD axes, KR-CAP PhoX and KR-CAP PhoA; KR-CAP PhoX and KR-CAP PhoA. The correlation coefficients are colored according to their values; being blue the positives values and red the negative values. b) Correlogram of the acid phosphatases displays the Pearson correlation coefficients between KR-CAP Nsap-A axes, KR-CAP Nsap-B and KR-CAP Nsap-C; KR-CAP Nsap-B and KR-CAP Nsap-C. The correlation coefficients are colored according to their values; being blue the positives values and red the negative values. c) Correlogram of the phytases displays the Pearson correlation coefficients between KR-CAP BPP axes and KR-CAP CPhy. The correlation coefficients are colored according to their values; being blue the positives values and red the negative values. d) Correlogram of the most abundance displays the Pearson correlation coefficients. The correlation coefficients are colored according to their values; being blue the positives values and red the negative values. Correlation analysis and graphics were performed with cor R package.

Correlation matrix of KR-CAP axes. a) Correlogram of the alkaline phosphatases displays the Pearson correlation coefficients between KR-CAP PhoD axes, KR-CAP PhoX and KR-CAP PhoA; KR-CAP PhoX and KR-CAP PhoA. The correlation coefficients are colored according to their values; being blue the positives values and red the negative values. b) Correlogram of the acid phosphatases displays the Pearson correlation coefficients between KR-CAP Nsap-A axes, KR-CAP Nsap-B and KR-CAP Nsap-C; KR-CAP Nsap-B and KR-CAP Nsap-C. The correlation coefficients are colored according to their values; being blue the positives values and red the negative values. c) Correlogram of the phytases displays the Pearson correlation coefficients between KR-CAP BPP axes and KR-CAP CPhy. The correlation coefficients are colored according to their values; being blue the positives values and red the negative values. d) Correlogram of the most abundance displays the Pearson correlation coefficients. The correlation coefficients are colored according to their values; being blue the positives values and red the negative values. Correlation analysis and graphics were performed with cor R package.

191x271mm (300 x 300 DPI)

- 1
- 2
- 3
- 4
- 5
- 6
- 7
- 8
- 9
- 10
- 11
- 12
- 13
- 14
- 15
- 16
- 17
- 18
- 19
- 20
- 21
- 22
- 23
- 24
- 25
- 26
- 27
- 28
- 29
- 30
- 31
- 32
- 33
- 34
- 35
- 36
- 37
- 38
- 39
- 40
- 41
- 42
- 43
- 44
- 45
- 46
- 47
- 48
- 49
- 50
- 51
- 52
- 53
- 54
- 55
- 56
- 57
- 58
- 59
- 60

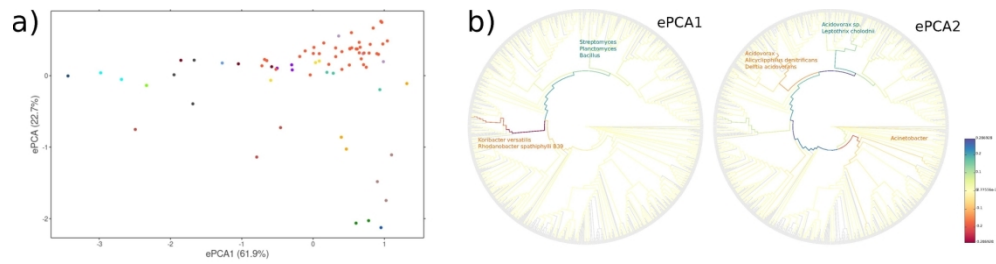


Figure 4: a) Graphic representation of the first two axes of the edge-PCA for PhoD using samples as observations. Each point represents samples from the project mpg1992 (blue); mpg3520 (green); mpg5588 (dark red); mpg7792 (gray); mpg8624 (mustard); mpg9904 (violet); mpg10450 (dark blue); mpg10523 (stone blue); mpg10541 (turquoise); mpg10956 (yellow); mpg13011 (lilac); mpg13520 (jade); mpg13948 (orange); mpg20922 (brown); mpg89409 (brick-red); mpg91922 (light green); mpg93346 (light blue). b) The phylogeny distribution of PhoD hits along the first and second axis of the analysis (protein with positive coefficients are marked in blue and proteins with negative coefficients are marked in orange). The edge-PCA was performed using gappa software and tree and domain composition diagrams were drawn using Archaeopteryx (<https://sites.google.com/site/cmzmasek/home/software/forester>).

a) Graphic representation of the first two axes of the edge-PCA for PhoD using samples as observations. Each point represents samples from the project mpg1992 (blue); mpg3520 (green); mpg5588 (dark red); mpg7792 (gray); mpg8624 (mustard); mpg9904 (violet); mpg10450 (dark blue); mpg10523 (stone blue); mpg10541 (turquoise); mpg10956 (yellow); mpg13011 (lilac); mpg13520 (jade); mpg13948 (orange); mpg20922 (brown); mpg89409 (brick-red); mpg91922 (light green); mpg93346 (light blue). b) The phylogeny distribution of PhoD hits along the first and second axis of the analysis (protein with positive coefficients are marked in blue and proteins with negative coefficients are marked in orange). The edge-PCA was performed using gappa software and tree and domain composition diagrams were drawn using Archaeopteryx (<https://sites.google.com/site/cmzmasek/home/software/forester>).

171x77mm (300 x 300 DPI)